Doctoral Thesis

Almost Periodic Frequency Arrangement and Its Applications to Communications

Isao NAKAZAWA

Graduate School of Informatics, Kyoto University

March 2020

Preface

Extensive communication and information services for connections and data processing are being developed not only for person to person, but also for machine to machine communication. This is accompanied by rapidly inclrease in the data content, transmission terminals, and the swift expansion of the application industry. In near future, the multi-layered networks, heterogeneous networks, and the seamless networks are expected to form the communication system infrastructures.

5G mobile communications systems mainly adopt the orthogonal frequency division multiplexing (OFDM) on the downlink from the base stations to the mobile users and the orthogonal frequency division multiple access (OFDMA) for user access because of its efficient use of frequency. Additionally, the OFDM scheme is applied to the IEEE 802.11 LAN, broadcasting, etc. for interference suppression and frequency efficiency.

However, as the number of users increases, the number of subcarriers also increases, and the subcarrier interference by the orthogonal multiplexing scheme loses the benefits of the OFDM or OFDMA scheme because of the frequency shift at the millimeter frequency bands and the narrower subcarrier frequency intervals.

Recently, chaotic spreading codes generated by almost periodic functions were reported to be advantageous in super multi-access. Additionally, simulation results for its applicability to mobile and satellite communications have also been reported. It has been found that the almost periodic frequency arrangement (APFA) has different characteristics as compared to those of the existing periodic signals. We have been continuously reporting on the applicability of the APFA system in the mobile and satellite communication systems. In studies related to the chaos theory, research regarding various communication systems has recently increased due to the features of constant power chaotic spreading and its security. Moreover, wideband radio communication systems are currently harnessing the asynchronous nature of signals.

This thesis aims to propose a new concept of communication methods and the basic configuration of new communication methods to respond to the increasing communications and number of devices in the twenty-first century. We also present the effective new technologies required for the solving problems.

The new concept of communication methods is wireless communication systems based on disjoint set of irrational numbers for frequency allocation which are completely different from existing communication systems that use the rational numbers to specify frequency. We have evaluated the applicability of this technology in comparison with existing communication systems .

An almost pediodic frequency arrangement (APFA) system is a type of frequency-division multiplexing method, which is constructed by the disjoint sets of irrational numbers for frequency allocation created using the power root of a prime number. In our simulation, it is assumed that the connection with more than *one million channels* at a base station is possible usng the super-multicarrier APFA systems with the same communication quality characteristics as the current system.

Futhermore, we found three types of probability mass function (PMF) distributions from the frequency spectrum analysis of the frequency deviation between the target frequency (rational number) and almost periodic function frequency (APFF). These three types correspond to the $1/f^A$ type probability density function by using computer simulations. Because these three types of $1/f^A$ probability density functions have already been observed in the electronic circuit of the wireless communication system, the APFA system can provide a communication scheme that reflects the influence of noise received under the actual communication environment.

To study the chaotic features of base-band signals of APFA, a new frame Lyapunov exponent (FLE), which estimates the phase difference sensitivity depending on the frame number, is proposed. This means that the APFA is a kind of chaotic communication system that utilizes a chaotic frequency hopping mechanism due to the periodicity of almost periodic frequency allocation. The universal feature of FLE is to elucidate several characteristics such as short-term radiations of phases.

Acknowledgements

First of all, the author wishes to express his sincere appreciation to Professor Ken Umeno, for his continuous support and guidance in the present work and his research. Without his persistent help and constant encouragement, this work would have never been completed.

The author would like to express his great gratitude to Professor Masahiro Morikura, Department of Communications and Computer Engineering, Graduate School of Informatics, Kyoto University.

The author would like to express his great gratitude to Professor Nobuo Yamashita, Department of Applied Mathematics and Physics, Graduate School of Informatics, Kyoto University.

The author would like to thank General Manager Dr. Morio Toyoshima, the laboratory head at National Institute of Information and Cmmunications Technology for helpful discussions.

The author would like to thank Dr. Kiyoshi Igarashi, Graduate School of Informatics, Physical Statistics Reserch Group, Kyoto University for comments on this paper.

Finally, I would like to thank my familiy for their support throughout my studies in Kyoto University.

Contents

List of Figures

List of Tables

Abbreviation

Abbreviation : Description
APFA : Almost Periodic Frequency Arrangement
APFAS: APFA Scheme
APFF : Almost Periodic Function Frequency
AWGN: Additive White Gaussian Noise
BER: Bit Error Rate
C-APFA: Chaos-APFA
CDMA: Code Division Multiple Access
EOM-OFC : Electro-Optics-Modulator-based Optical Frequency Comb
EIPR: Equivalent Isotropic Radiated Power
ETS-VIII: Engineering Test Satellite VIII “ KIKU No.8 ”
ETS-IX: Engineering Test Satellite IX
FFT: First Fourier Transform
FLE : Frame Lyapunov Exponent
GPS: Global Positioning System
LTE: Long Term Evolution
M2M: Machine to Machine
MER: Modulation Error Ratio
MIMO: Multiple-Input Multiple Output
MPA: Multiport Amplifier
NITR: Network Information Transmitter and Receiver
NOF: Normalized Offset Frequency
OFDM: Orthogonal Frequency Division Multiplexing
OFDMA : Orthogonal Frequency Division Multiple Access
QAM: Quadrature Amplitude Modulation
TFA: Target Frequency Arrangement
NGAT : Next Generation Access Technologies
PAPR: Peak-to-Average Power Ratio

Abbreviation : Description

PMF: Probability Mass Function

QPSK: Quadrature Phase-Shift Keying

SC-FDMA : Single-Carrier Frequency Division Multiple Access

ITU-R: International Telecommunication Union Radiocommunication sector

UWB: Ultra Wide Band

WINDS: Wideband Inter-networking Engineering Test and Demonstration Satellite

Chapter 1

Introduction

1.1 Background of the Study

Extensive communication and information services for connections and data processing are being developed not only for person to person communication, but also for machine to machine communication. This is accompanied by rapid increasing the data content, transmission terminals, and the swift grouth of the application industry. It was expected that the multi-layered networks, heterogeneous networks and the seamless networks will be the communication system infrastructures in the new era after 2020 [1]-[4].

5G mobile communications systems mainly adopt the orthogonal frequency division multiplexing (OFDM) on the downlink from the base station to the mobile users and the orthogonal frequency division multiple access (OFDMA) for user access because of its efficient use of frequency. Additionally, the OFDM scheme is applied to the IEEE 802.11 LAN, broadcasting, etc. for interference suppression and frequency efficiency.

However, as the number of users increases, the number of subcarriers also increases, and the subcarrier interference by the orthogonal multiplexing scheme loses the benefits of the OFDM or OFDMA scheme because of the frequency shift at the millimeter frequency bands and the narrower subcarrier frequency intervals.

Recently, chaotic spreading codes generated by almost periodic functions were reported to be advantageous in super multi access [5]-[8]. Additionally, simulation results for its applicability to mobile and the satellite communications have also been reported. It has been found that almost periodic frequency arrangement (APFA) has different characteristics in compared to those existing periodic signals. We have been continuously reporting on the applicability of the APFA system to mobile and satellite communication systems [12]-[17].

In studies related to chaos theory, research regarding various communication systems has recently increased due to the features of constant power chaotic spreading and its security. Moreover, wideband radio communication systems are currently harnessing the asynchronous nature of sequences. This study focuses on *asynchronous* multicarrier communication for frequency division multiplexing and multi-access. It is assumed that all frequencies for frequency allocation are designed using the Weyl uniform distribution and prime number theorems [9]-[11].

1.2 Wireless Communication Systems

1.2.1 New Concept of Wireless Communication Systems

This thesis aims to propose a new concept of wireless communication systems based on the disjoint sets of irrational numbers that can potentially avoid the degradation of radio wave environment, and to verify its applicability to typical communication systems.

The APFA system proposed here is constructed by disjoint sets of irrational numbers given by the power root of a prime number. Based on our simulations, it will be confirmed that it is possible to connect more than one million channels at a base station using the super-multicarrier APFA systems with the same communication quality characteristics as the current system.

Using computer simulations, the probability mass function (PMF) of frequency deviation between the target frequency and almost periodic function frequency (APFF) can demonstrate that it has three types of areas represented by $1/f^A$ type probability density functions for A=0, 1, and 2.

Since these three types of $1/f^A$ probability density function have already been confirmed in the electronic circuit of the wireless communication system, the APFA system can provide a communication scheme that reflects the influence of noise received under the actual communication environment.

In chaotic feature of APFA, a frame Lyapunov exponent (FLE) which can estimate the phase difference sensitivity depending on the frame number is newly proposed in Chapter 4.
We reveal the universal feature of FLE and elucidate several characteristics such as short-term radiations of phases.

Figure 1.1 shows the target of subcarrier number of super-multicarrier APFA in this thesis and the subcarriers number of IEEE 802.11 LAN, 4G LTE / LTE-Advanced wireless mobile communications, and 5 Generation mobile communications systems, and digital terrestrial television broadcasting.

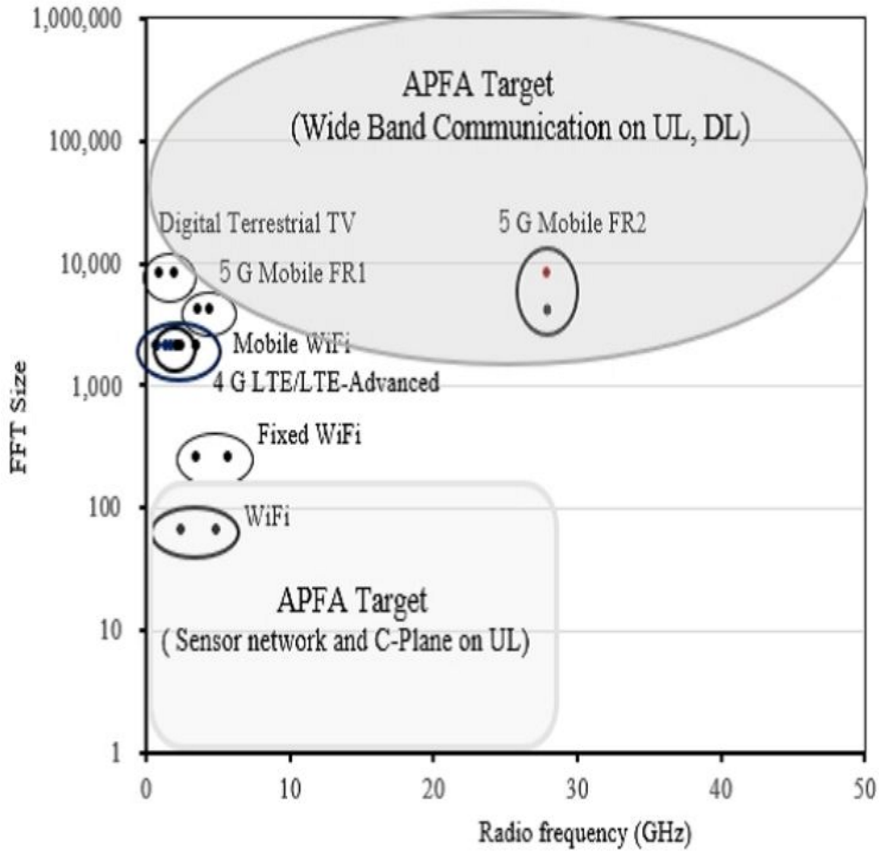

Figure 1.1: Comparison of the number of subcarriers with the other methods,
APFA Target: Radio Frequency greater than 100 MHz,
5G Mobile FR1: 5Generation Mobile Communications Systems on frequency band (450-6000 MHz) [1] [2],
5G Mobile FR2: 5Generation Mobile Communications Systems on frequency band (24.25-52.6 GHz) [1] [2],
4G LTE/LTE-Advanced: 4G LTE/LTE-Advanced Wireless Mobile Communications [2],
Fixed WiMAX: IEEE 802.16d on 3.5 and 5.8 GHz bands,
Mobile WiMAX: IEEE 802.16e-2005 on 2.3, 2.5 and 5.8 GHz bands,
WiFi: IEEE 802.11ax on 2.5 and 5 GHz bands,
Digital Terrestrial TV: Digital Terrestrial Television Broadcasting on 470-710 MHz) [3] [4],
UL: Up Link,—— DL: Down Link.

1.2.2 Satellite Communication

This section outlines the present state and future trends of fixed satellite systems on International Telecommunication Union Radiocommunication Sector (ITU-R) standardizations and in which the NICT (National Institute of Information and Communications Technology, Japan) was proceeding with the test and development.

1.2.2.1 International Telecommunication Union Radiocommunication

In International Telecommunication Union Radiocommunication Sector (ITU-R) use cases in satellite communication are classified into four cases in a report (Recommendation ITU-R M.2083) under deliberation on the integration of satellite and 5G. Table 1.1 shows the four cases in integration of satellite systems into next generation access technologies (NGAT).

Table 1.1: Satellite use cases for integration of satellite systems into NGAT
(Cited from Report ITU-R M.2460-0 Key elements for integration for integration of satellite systems into next generation access technologies).

Use cases	Examples	Number of sites	Note
Trunking and head-end feed	Service to remote areas; special events	Limited to unserved areas in a carrier ' s network	Fig. 1.2
Backhauling and Multicasting tower feed	Surge capacity to overloaded cells, plus content delivery (e.g. video) to local caches; efficient broadcast service to end users	Thousands	Fig. 1.3
Communications	In Flight Connectivity for Aircraft; on move to land vehicles; broadband to ships and trains	Potentially millions connectivity directly	Fig. 1.4
Hybrid multiplay	Video and broadband connectivity directly to home or multi tenant building with NGAT distribution in building	Potentially millions	Fig. 1.5

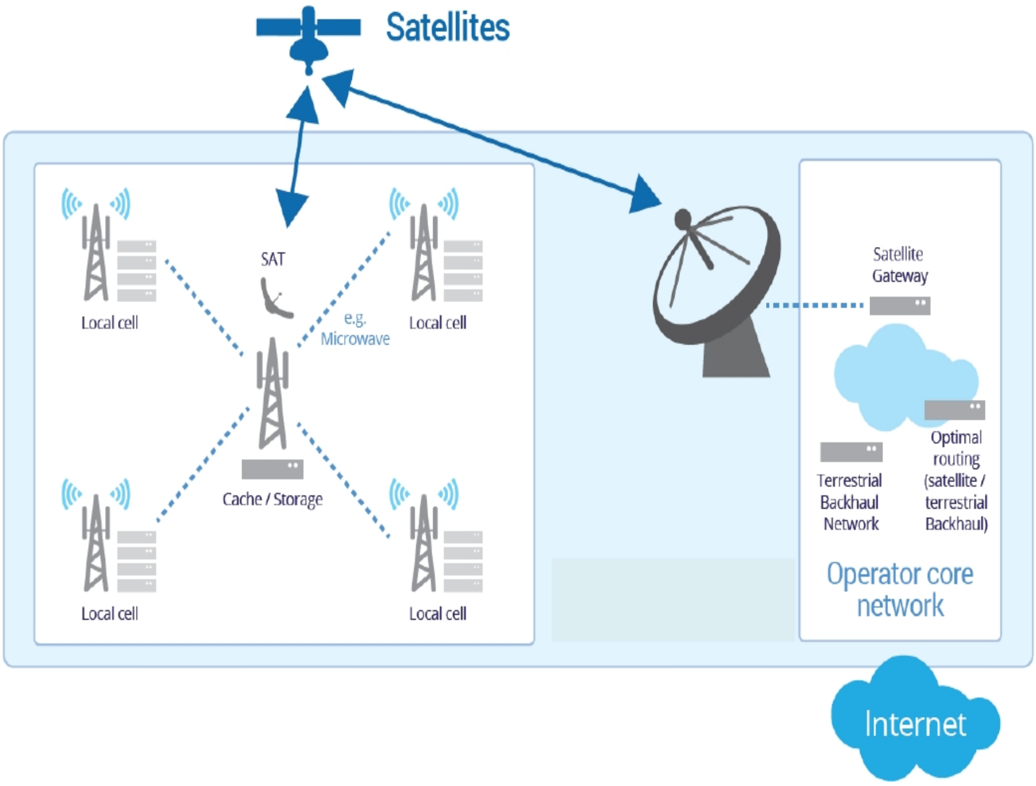

Figure 1.2: Representative diagram of the Trunking and Head-end Feed use case
(Cited from Report ITU-R M.2460-0 Key elements for integration for integration of satellite systems into Next Generation Access Technologies).

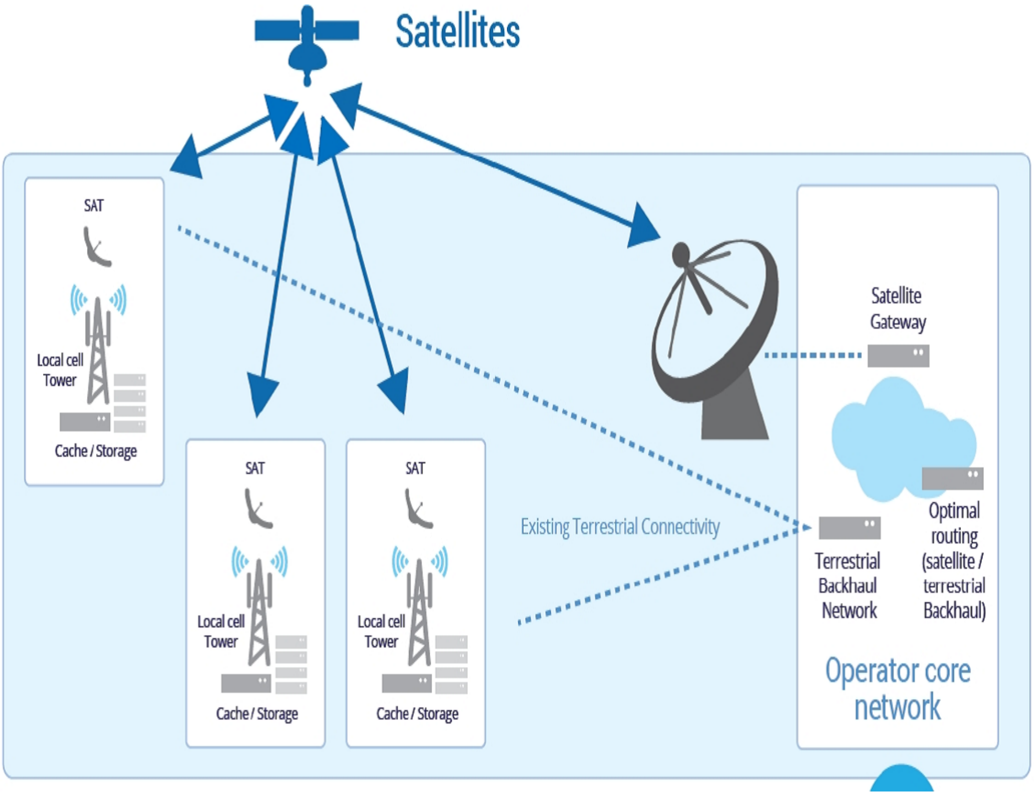

Figure 1.3: Representative diagram of the backhauling and multi-casting Tower Feed use
(Cited from Report ITU-R M.2460-0 Key elements for integration for integration of satellite systems into next generation access technologies).

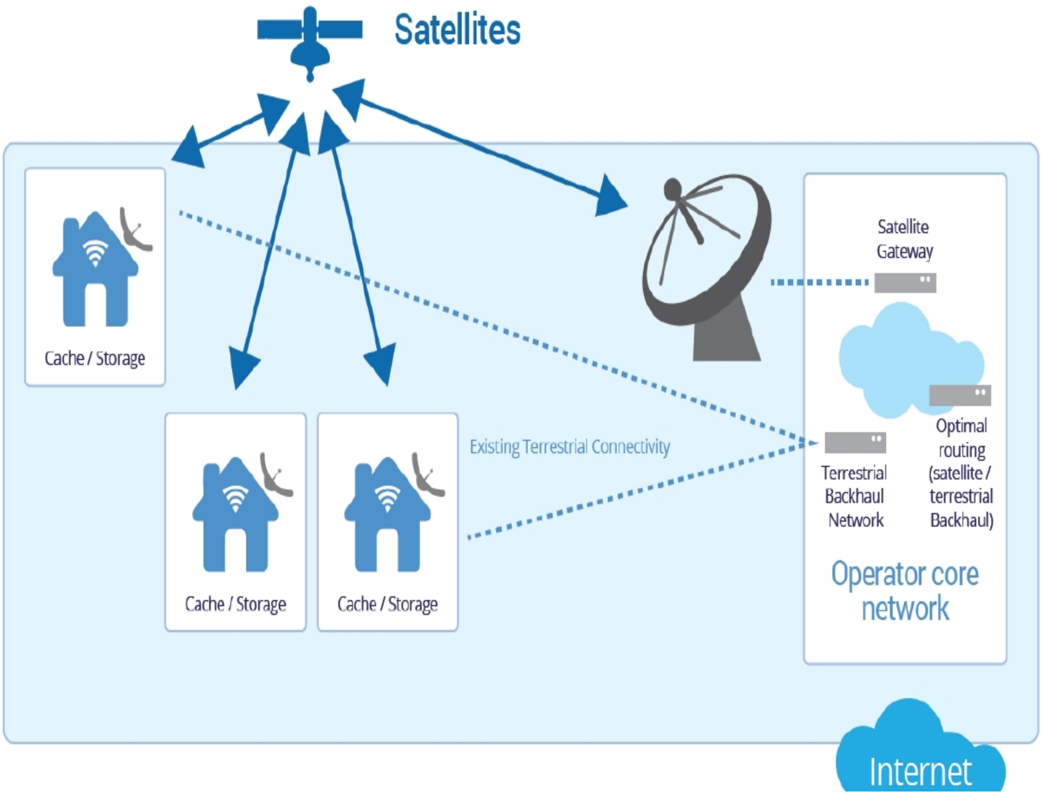

Figure 1.4: Representative diagram of the communications on the move use case
(Cited from Report ITU R M.2460 0 Key elements for integration for integration of satellite systems into next generation access technologies)

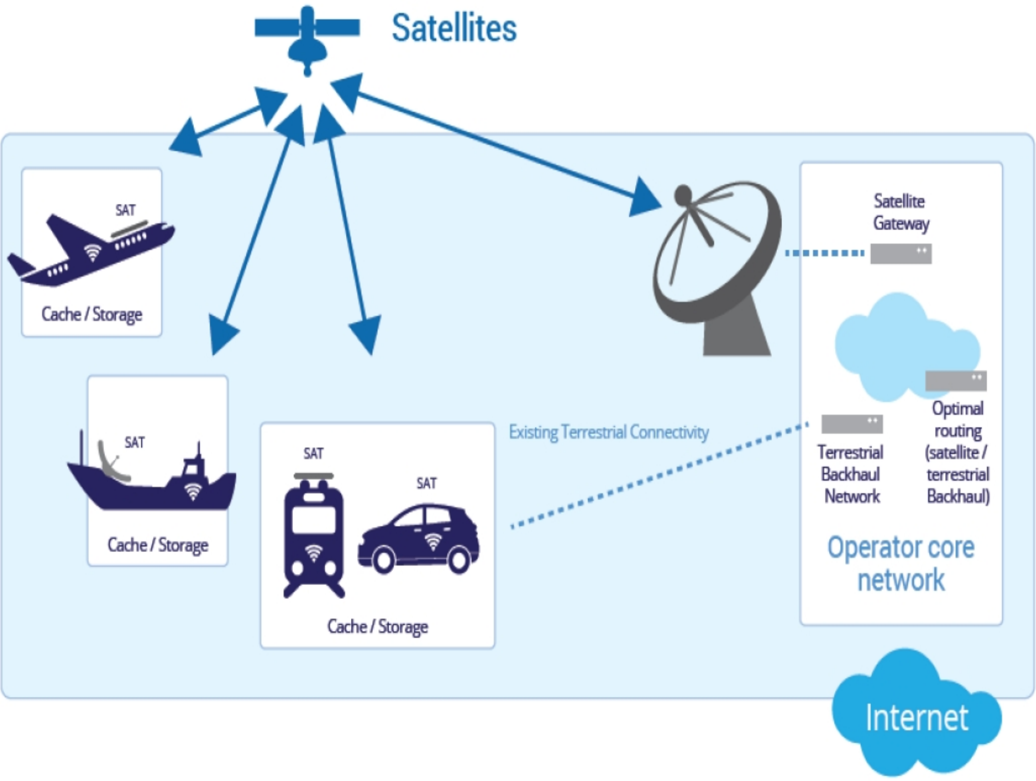

Figure 1.5: Representative diagram of the hybrid multiplay use case
(Cited from Report ITU-R M.2460-0 Key elements for integration for integration of satellite systems into next generation access technologies).

1.2.2.2 Engineering Test Satellite VIII

The mobile satellite communication experiments using the Engineering Test Satellite VIII, which was launched in December 2006, have been conducted for duration of approximately six years. The performance evaluation tests for onboard equipment, earth stations and mobile satellite communication systems have been conducted, in additionto application experiments [37].

A diagram of the ETS-VIII in orbit is shown in Fig. 1.6, and its main specifications are provided in Table 1.2. Table 1.3 shows principal particulars of the communication mission.

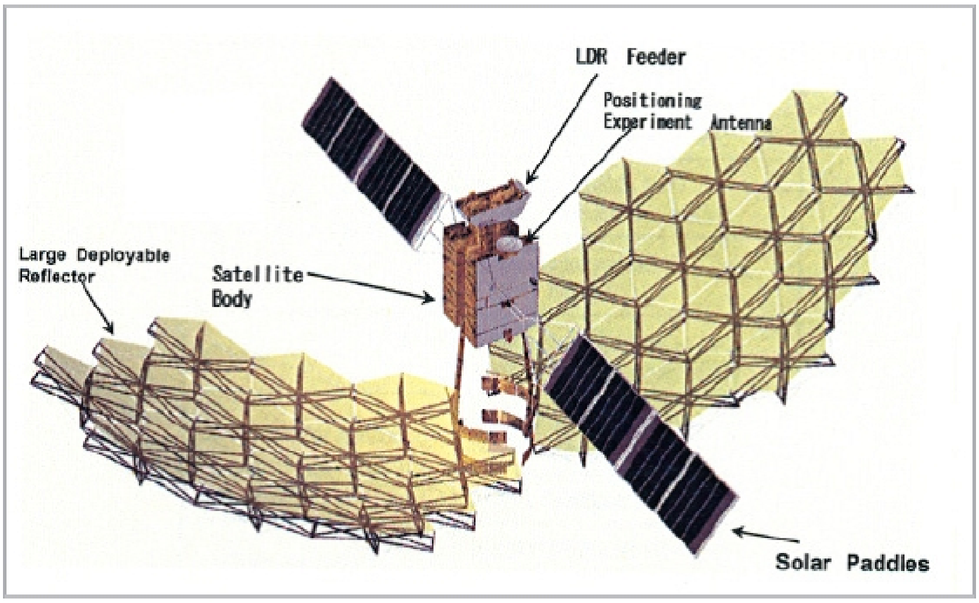

Figure 1.6: Diagram of the Engineering Test Satellite (ETS-VIII) in orbit
(Cited from Overview of Mobile Satellite Communication Experiments using the ETS-VIII).

Table 1.2: Main specifications of the Engineering Test Satellite (ETS-VIII)
(Cited from Overview of Mobile Satellite Communication Experiments using the ETS-VIII).

Items	*Characteristics*
Launch Year	JFY2004 Launched by H-IIA204 at Tanegashima Space Center
Design Life	10 years (Satellite Bus) 3 years (Mission Equipment)
Orbit	Geostationary orbit (146° East)
Weight	3,000kg (at beginning of life) 1,200kg (mission equipment)
Electric Power generated	7,500W (summer solstice, 3 years after launch)
Attitude Control	3-Axis Stabilized
Attitude Accuracy	$\pm 0.05 \circ$ (Roll/Pitch) $\pm 0.15 \circ$ (Yaw)

Table 1.3: Principal Features of Engineering Test Satellite VIII
(Cited from Overview of Mobile Satellite Communication Experiments using the ETS-VIII).

Items	*Characteristics*
Orbit	Geostationary orbit, 146 degrees East
Frequency	S-band (2.6 / 2.5 GHz) for mobile link Ka-band (30 / 20 GHz) for feeder link
Antenna	13 m mesh deployable reflectors for mobile link 0.8 m offset parabola for feeder link
Tx power	400 W for S-band 8 W for Ka-band
Onboard switch	Circuit switch for personal communications Packet switch for mobile communications for Ka-band
Data Rate	Voice 5.6 kbps Data 32 kbps Packet -1,024 kbps Broadcast 2 20 kbps $\times$ 6 ch (OFDM)
MOD Access Method	Communication $\pi/4$ QPSK MC-TDMA Packet $\pi/4$ QPSK Slotted ALOHA Reserved Broadcast $\pi/4$ QPSK OFDM, and so on

1.2.2.3 Wideband InterNetworking engineering test and Demonstration Satellite (WINDS)

NICT established the concept of the "Gigabit Satellite" and began studying the feasibility to realize a high-data-rate satellite communication system in fiscal year 1992. Figure 1.7 is a schematic diagram of WINDS applications to increase the usability of satellite communications, particularly in ensuring communications in disasters [36]. WINDS main specifications related to the satellite are provided in Table 1.4. Table 1.5 shows principal particulars of the communication mission.

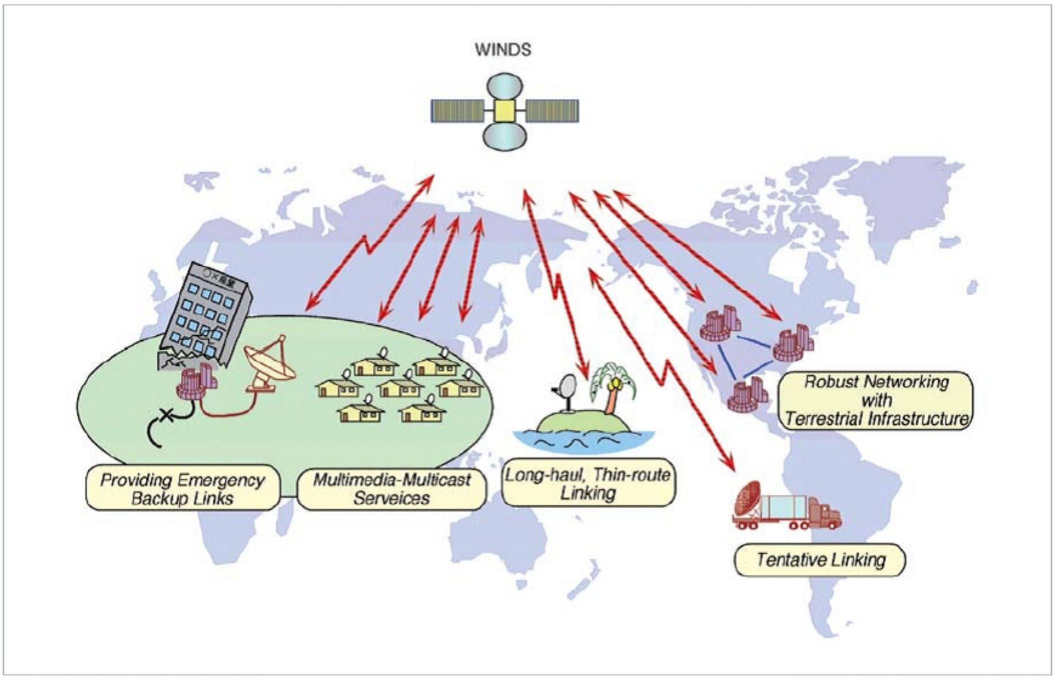

Figure 1.7: Schematic diagram of WINDS applications
(Cited from Journal of the National Institute of Information and Communications Technology Vol.54 No.4 2007)

Table 1.4: Main specifications of WINDS
(Cited from Journal of the National Institute of Information and Communications Technology, Vol.54 No.4 2007)

Items	*Characteristics*
Launch Year	JFY2007 (Feb. 2008)
Mission Life	5 years
Location	Geostationary orbit (143° East)
Mass	4,850kg (Lift off)
Electric Power generated	>5,200W (EOL, summer solstice)
Consumption Power	8,000W (EOL, summer solstice, AJT) 4,000W (Eclipse)
Attitude Control	Zero-Momentum 3-Axis control $\pm 0.05 \circ$ (Roll/Pitch) $\pm 0.15 \circ$ (Yaw)

Table 1.5: Major specifications of communication mission
(Cited from Journal of the National Institute of Information and Communications Technology, Vol.54 No.4 2007)

Items	Major specifications
Orbit	Geostationary orbit, 143 degrees East
Frequency band	TX : 17.7 ~18.8 GHz RX : 27.5 ~28.6 GHz
Antenna type	Aperture diameter: 2.4m Offset Casegrain
Number of beams	Japan and neighboring countries: 12 South east Asia: 7
G/T	approx. 18 dB (at beam edge and maximum MPA output)
EIRP	approx. 70 dBW (at beam edge and maximum MPA output)
NITR	Modulation PCM(NRZ-L)/PSK/PM Sub-carrier UL : 16 kHz DL ; 40 kHz Modulation index ≤ 1.1 rad $\pm 10\%$ Data rate UL : 4 kbps DL : 10 kbps

Note :

MPA: multiport amplifier

NITR: Network manegement information transmitter and receiver,

UL: Upper Link,

DL: Down Link

1.2.2.4 System Requirements

The system requirements for that WINDS satellite systems are as follows:
(1) User should be able to access services anywhere, anytime.
(2) Combination of different fixed, terrestrial and satellite networks.
(3) Heterogeneous networks with interoperability capacity to provide ubiquitous networking.
(4) Seamless network.
(5) Peak to Average Power Ratio (PAPR).
(6) Frequency efficiency.

We study APFA method from the veiw point of the above conditions.

1.2.3 Mobile Communication

1.2.3.1 5G System

Mobile radio communications in domestic systems have been introduced every 10 years since commercialization (1979) and have been experiencing remarkable development. The fourth generation, called LTE-Advanced, which is an extension of LTE (Long Term Evolution of IMT2000) from the third generation CDMA system (IMT2000), adopts OFDM / SC-FDMA system. Furthermore, the fifth generation mobile communication system (5G systems) is being promoted in the world with the aim of the start of the service in 2020 (Japan) while maintaining compatibility with LTE.
Figure 1.8 shows the relative comparisons to important system specifications table of the division multiplexing systems for each generation of mobile communicationto compare with APFA system for discussion in the present thesis.

Division multiplexing	MODEM	Mobile system	Multiple access	Multi-plexing	Band width	PAPR	Power efficiency
TDMA	BPSK QPSK NQAM	2nd Generation Mobile	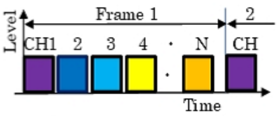	Small scale	○	○	○
CDMA	CDM	3rd Generation Mobile	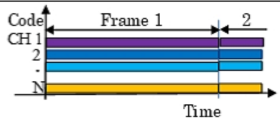	Small scale 64 CH	○	○	○
OFDMA	BPSK QPSK NQAM	4th, 5th Generation Mobile	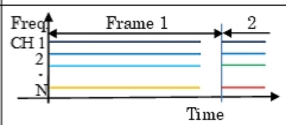	Mid-size 2014 CH	◎	×	×
APFA	BPSK QPSK NQAM	6th or beyond Generation Mobile	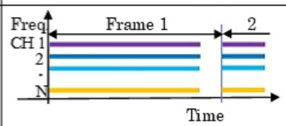	Large scale 1,000,000 -64 CH	◎	Large scale : × Small scale: ◎	Large scale : × Small scale: ◎
SC-FDMA	BPSK QPSK NQAM	4th, 5th Generation Mobile	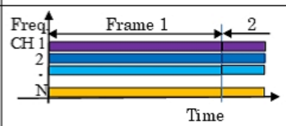	Small scale	△	×	×

Figure 1.8: Important system specifications for n-th mobile systems to compare with APFA.

Note:

This symbol ◎ denotes best performance,

This symbol ○ denotes better performance,

This symbol △ denotes good performance,

This symbol × denotes bad performance in each category.

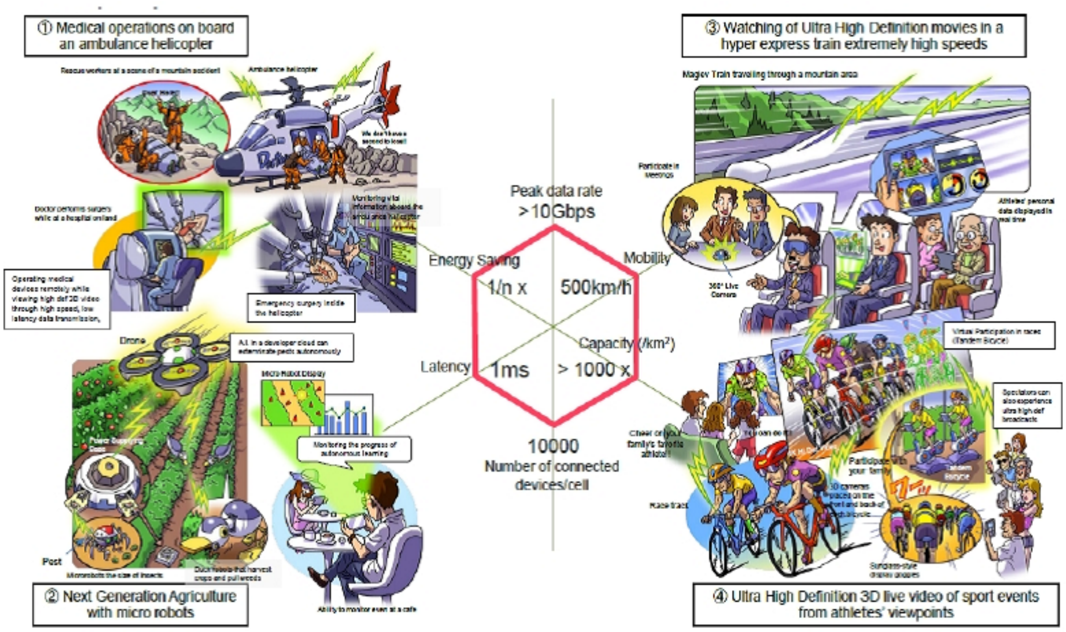

Figure 1.9: Crossover collaboration for fruitful 5G eco-society (Cited from 5GMF: White paper Version 1.1).

Frequency bands which have Levels 3 and 4 for sharing possibility are considered as the preferred bands for 5G as shown in Tables 1.6-1.8. This is the result of stage 2 evaluation process of MIC.

Note:

Stage2: Evaluation from inter system point of view.

Level 3 : Possible for sharing under certain conditions and worth considering for sharing.

Level 4 : Possible for sharing.

Table 1.6: Results of Stage2 (6-30GHz)
(Cited from 5GMF: White paper Version 1.1).

Frequency Band (GHz)	Bandwidth (GHz)	Level of sharing possibility
5.925-7.25	1.325	3, 4
7.375-8.75	1.375	3, 4
10-10.5	0.5	3
10.55-10.68	0.13	3
10.7-11.7	1.0	3
14.5-15.35	0.85	3
15.4-21.4	6.0	3, 4
22-23.6	1.6	3
24.75-31	6.25	3, 4

Table 1.7: Results of Stage2 (30-60GHz)
(Cited from 5GMF: White paper Version 1.1).

Frequency Band (GHz)	Bandwidth (GHz)	Level of sharing possibility
31-31.3	0.3	4
31.5-42.5	11	3, 4
45.3-47	1.7	4
47-50.2	3.2	3, 4
50.4-52.6	2.2	3, 4
54.25-57	2.75	3

Table 1.8: Results of Stage2 (60-100GHz)
(Cited from 5GMF: White paper Version 1.1).

Frequency Band (GHz)	Bandwidth (GHz)	Level of sharing possibility
66-76	10	3, 4
81-86	5	3
92-100	8	4

1.2.3.2 System Requirements

The requirements on a 5G system are as follows :
(1) Peak data rate must be more than 10 Gbps.
(2) Mobility more than 500 km/h with latency 1 msec.
(3) Maximal number of connected devices per km^2 is more than 1 million
(4) Capacity per unit area of 1000 times larger as compared to 4G.
(5) Significant reduction of power consumption.

The requirements on 5G network and technology considering satellite system are as follows :
(1) Seamless network,
(2) Heterogeneous networks with interoperability capacity to provide ubiquitous,
(3) Peak to Average Power Ratio (PAPR),

Figure 1.9 shows typical usage scenarios by using comprehensive illustrations .

1.3 Communication Environment

In Fig, 1.10, we show the frequency characteristics of the phase noise (dBc / Hz) at 1 kHz offset frequency for the typical radio frequency (RF) band oscillators based on the commercial products data noise and development results of phase noise [18,19]. There, the RF band oscillators that are selected from general device makers are crystal oscillator, atomic oscillator used for a global positioning system (GPS), EOM-OFC (electro-optics-base optical frequency comb) with improved phase noise at high frequencies and frequency synthesizer used for a measuring instrument. Since the octave of the RF frequency is assumed to increase the phase noise of the multiple wave by 6 dB, the frequency characteristics of phase noise in Fig. 1.10 are extended by 6 dB per octave from the oscillation frequency of the oscillator.

In Fig. 1.11, we shows phase noise at near frequency to the oscillation frequency for the same oscillator shown in Fig. 1.10. The phase noise increases in a form $1/f^A$ with $A > 0$ as the offset frequency decreases. As shown in Fig. 1.10 and Fig. 1.11, the subcarrier always has phase noise in the actual communication environment [19]. However, when the number of subcarriers is low and the radio frequency band is low, it is not noticeable.

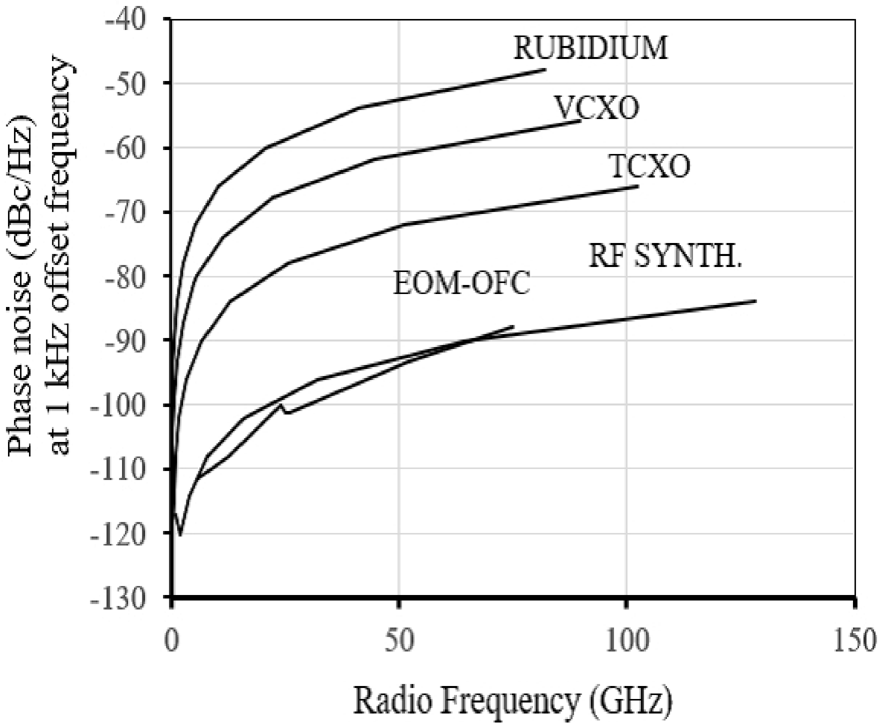

Figure 1.10: Various phase noise (dBc/Hz) at 1 kHz offset frequency as copared to ratio frequency (GHz).
EOM-OFC: Electro-optics-modulation-based optical frequency comb. [18],
TCXO: Temperature compensated crysatal oscillator, (Company A),
VCXO: Power control crystal oscillator, (Company A),
RUBIDIUM: Atomic Clock, (Company B),
RF SYNTH: RF synthesizer, (Company C).

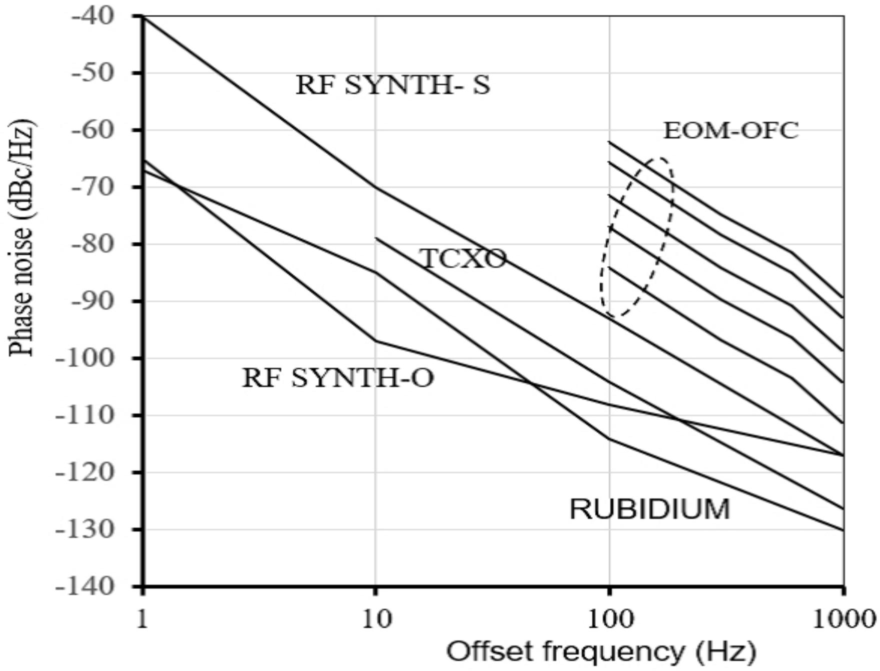

Figure 1.11: Phase noise (dBc/Hz) as compared to offset frequency
EOM-OFC: Eelectro-optics-modulation-based optical frequency comb. at 6 GHz to 72 GHz frequency [18],
TCXO: Temperature compensated crysatal oscillator at 150 MHz, (Company A),
RUBIDIUM: Atomic Clock at 10 MHz, (Company B),
RF SYNTH-S: Standard RF synthesizer at 1 GHz, (Company C),
RF SYNTH-O: At 1 GHz, OCXO type RF synthesizer (Company C).

1.4 Chaotic Spread Spectrum Method

The constant power chaotic spreading codes have the feature of lower PAPR as compared to OFDM (Orthogonal Frequency Division Multiplexing), and the application studies to various communication systems are reported [5-8]. The constant power chaotic spreading code systems are suitable in the satellite communication systems from the view point of frequency effective utilization.
Here, we introduce the following chaos codes (Primitive root Chaos Code, 2D Exactly Solvable Chaos, Almost Periodic Function Code) for wideband radio communication systems as well as the satellite communication systems.
A Primitive Root Chaos Code [5] (Umeno, 2008)
Primitive root code is given by the equation as follows:

$$PC(p, q, k) = e^{j2\pi \cdot \frac{q^k \bmod p}{p}}, \tag{1.1}$$

where p is the prime and q is the primitive root, and parameter k should be an integer satisfying,

$$0 \leq k \leq p - 2. \tag{1.2}$$

In addition, it is reported that they are mutually orthogonal for different $k(0 \leq k \leq$p$-2)$ [5]. The constellation map in the case of (p, q)= (1217,576) is shown in Fig. 1.12 as one example.

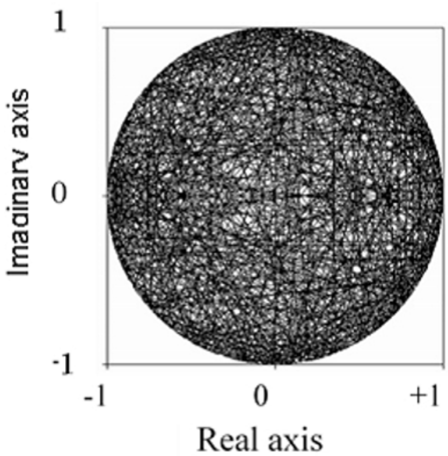

Figure 1.12: The constellation map of the primitive root code at (p, q)= (1217,576).

B 2D Exactly Solvable Chaos

The 2D Exactly Solvable Chaos (Two dimensional exactly solvable chaos) is introduced by addition theorem of a complex exponential function $e^{j\theta}$, real part x and imaginary part y by the equation as follows [5][6][41]:

$$(x_n, y_n) = (\cos m^{n-1}\theta, \sin m^{n-1}\theta), \quad \text{where } m \text{ is an integer such that } m \geq 2. \tag{1.3}$$

Since Eq. (1.3), Eq. (1.4), and Eq. (1.5) can be seen as a two dimensional mapping with m = 2, the general solution can be represented by Eq. (1.3). Here, the two dimensional mapping is given by: $x_{n+1} = f(x_n, y_n), y_{n+1} = g(x_n, y_n)$ where

$$f(x, y) = 2x^2 - 1, \tag{1.4}$$

$$g(x, y) = 2xy. \tag{1.5}$$

Here, from the equation $x_n^2 + y_n^2 = 1$, the constant power is ensured. In addition, x series and y series are orthogonal to the characteristics of the correlation function. The constellation maps in case of m=2-4 are shown in Fig. 1.13.

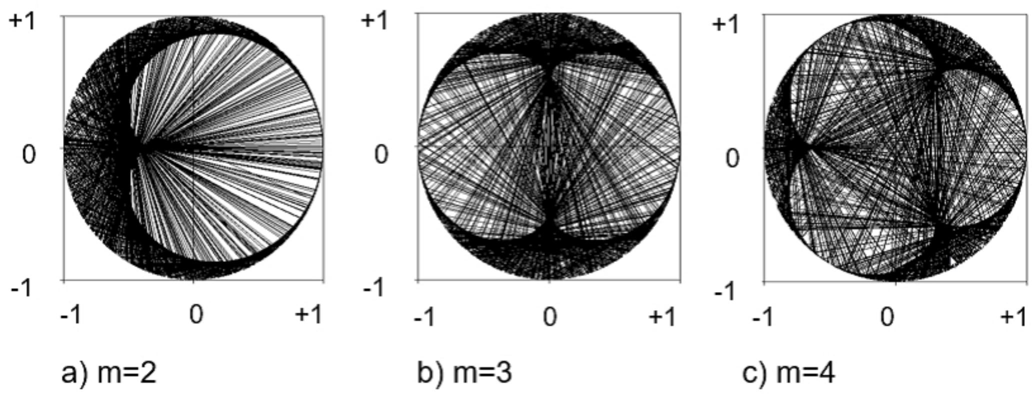

Figure 1.13: 2D exactly solvable chaos constellation map.

C. Almost Periodic Function Code

Almost periodic functions introduced in 1924 by H. Bohr are proposed to be applied to the communication. The fractional part of integral multiples of the root of prime numbers is assured to be distributed uniformly due to "Uniform distribution theorem" (equidistribution theorem) proven by Weyl in 1919 [9].

$$w(n) = re^{j2\pi\sqrt{p}x(mod1)}. \tag{1.6}$$

The normalized correlation between the sequences expected from that order of the relatively small error using the Weyl sequence such as the above $w(n)$. Almost periodic functions can be thus infinitely generated because the number of prime numbers is infinity. The constellation map calculated from the root of prime number 991 is shown in Fig. 1.14 as an example.

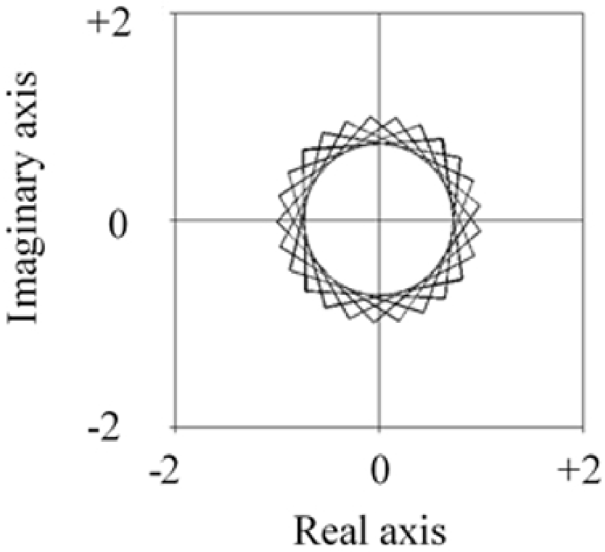

Figure 1.14: Constellation map for the root of prime number 991.

1.5 APFA Method and its Trends

Orthogonal frequency division multiplexing (OFDM), which is applied to 3G and 4G mobile communication, IEEE 8.2 LAN, broadcasting, and the like, is widely adopted from the viewpoint of suppression of multipath interference and frequency efficiency.

However, since the orthogonality and synchronization of codes are used to the maximum extent, it is pointed out that if the ideal synchronization and the orthogonality are inevitably lost, the code reproduction is greatly deteriorated.

The mobile communication system has been progressing almost every 10 years. Since around 2000, the third generation CDMA system has been introduced since around 2010, and OFDM system with combining new technology of multiple-input multiple output (MIMO) have been introduced, and the performance has been greatly improved by the introduction of OFDM system with new technology of multiple-input multiple output (MIMO), and its performance has been greatly improved until 2020.
5G is planned to become a star in Japan since 2020, and various services with air interface such as OFDMA (orthogonal frequency division multiple access), SC-FDMA (single-carrier frequency division multiple access), and massive MIMO have become available. In Japan, the ETS-VIII test satellite was launched in 2006. In the telephone class, mobile satellite satellites were tested and in 2008, the WINDS satellite was launched, and the high-speed communication test of the Gigabit class was advanced. The ETS-IX test satellite has been planned as a successor to ETS-VIII test satellite, and the cooperation with the mobile communication after the fifth generation mobile system at the ground system is also considered from the viewpoint of the future ninth test satellite. In the research and development of the APFA system, an extension of the application study the communication of the chaos CDMA system, the power constant chaos code and the approximate frequency function is given, and the basic concept of APFA is constructed from almost periodic functions, and the mobile communication APFA system is studied from the standardization of the mobile communication, and the satellite the viewpont of APFA method is studied from the test

operation of the satellite communication. Figure 1.15 shows our vision on the trends of the R & D surrounding mobile communications services, domestic technology satellite communications projects, and APFA.

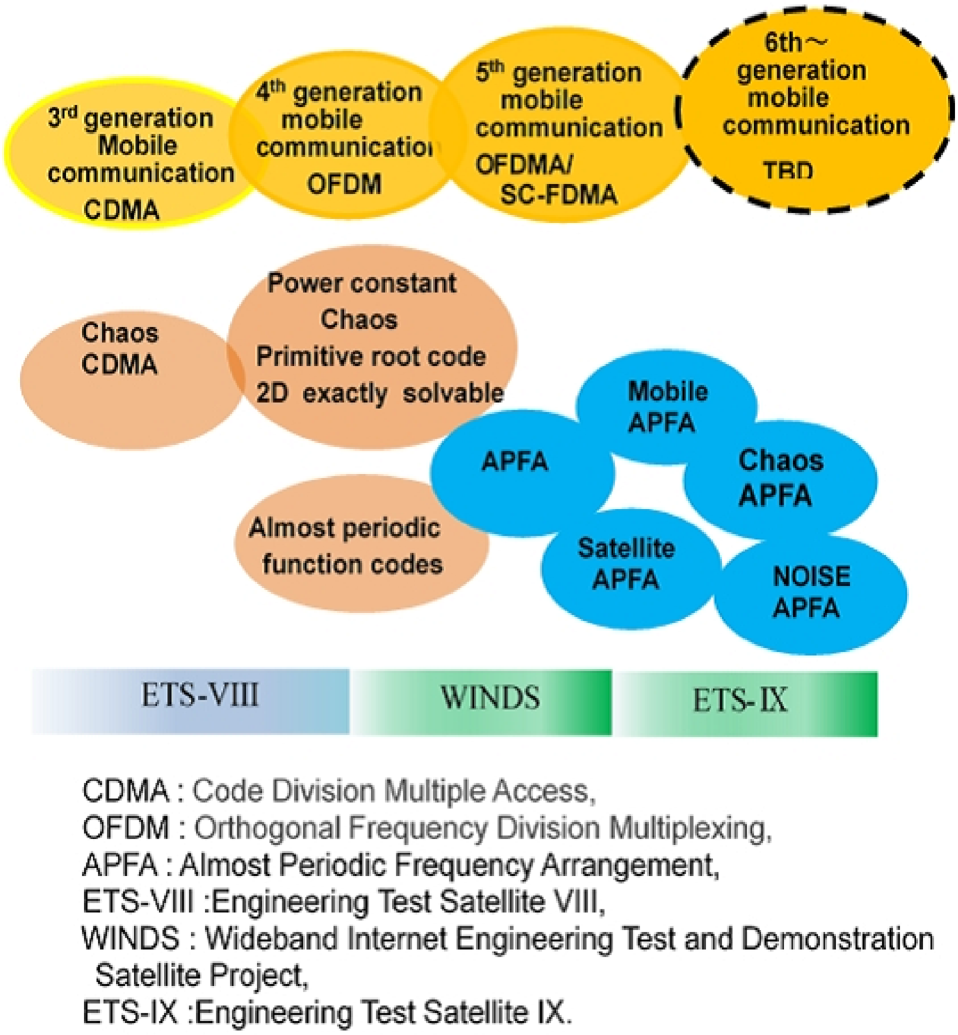

Figure 1.15: Our vision on the trends in research and development around APFA.

1.6 Composition of this Thesis

In this thesis, we first describe the basic concept of an APFA system based on a disjoint sets of irrational numbers given by the power root of the prime number.

In Chapter 2, we propose an APFA scheme using an irrational num-

ber group whose uniformity is guaranteed by the Weyl uniform distribution theorem.
In Chapter 3, we propose the implementation of APFA in an asynchronous communication mobile for satellite communications using high-frequency multiplexing based on a computer simulation system. We also present a new concept of APFA that can realize supermultiplexing and ultrawide band communication of up to *one million channels* and its basic performance computed by simulations is presented.
In Chapter 4, we propose a new frame Lyapunov exponent (FLE), which can estimate the phase difference sensitivity depending on the frame number in the APFA to capture chaotic feature of APFA baseband signls. We propose chaos-APFA (C-APFA) system using 2D exactly solvable chaos code to aim the optical communication system or THz radio communication system. We also a show new concept of C-APFA that enables subcarrier frequency allocation of up to *six million channels* and chaotic property using computer simulations.
In Chapter 5, we show the applications of APFA: Small Scale APFA, Seamless Satellite Communication System, and APFA UltraWide Band Wireless Communication (APFA-UWB). Chapter 6 summarizes this study.

Chapter 2

Basic Concept of Almost Periodic Frequency Allocation (APFA)

The OFDM system, which has been adopted by the current communication systems, has a frequency multiplexing of about up to 10000 channels, and it becomes difficult to cope with the demand for future ultrawide band communications. This chapter explains the description of the APFA method, which enables supermultiplexing of frequencies, and the features of the proposed method.

2.1 Fundamentals of APFA

While almost periodic functions (APF) was first introduced in the study of the spread spectrum scheme in 2014 [7], APF itself was already proposed in 1924, by H. Bohr as an extension of a conventional periodic function $|f(x+\tau) - f(x)| \leq \epsilon$, where f(x) is a complex function, x is a real parameter, and τ is a distance from x on f(x) that belongs to ϵ as a positive number.

In the case of $\tau \geq \epsilon > 0$, $f(x)$ corresponds to almost periodic functions. Moreover, the minimum value of the period τ is called the fundamental period. Multiple wave frequency is close to the base of the irrational numbers for different periods, which demonstrates a distinct APF. The fractional component of an integer multiple of the irrational number is uniformly distributed in (0, 1). It is based on the Weyl uniform distribution theorem (equidistribution theorem) [9]. The Weyl sequence using an irrational number generated from the power root of a prime number is expressed using the following equation in this study.

$$x\,(k,p,r) = \sqrt[k]{p}r \ (mod1), \tag{2.1}$$

where k is an index of power root, p is an arbitrary prime number $(2, 3, 5, 7 \cdots)$, N is a natural number, and r is a real number. We have selected prime numbers as an index to maintain the independency among the power root sequence of prime numbers.

The number $\pi(N)$ of prime numbers less than or equal to N is shown from the well-known prime number theorem $P_N \equiv \pi(N) \approx N/\mathrm{In}(N)$, where ln(N) is Napierian logarithm.

We define APFF (almost periodic functions frequency) $f_k(p_i)$ which transform by linear mapping of prime numbers as follows;

$$f_k(p_i) \equiv \sqrt[k]{p_i} \ \ (\text{ mod 1 }), \quad i = \mathit{1}, \mathit{2}, \cdots I, \tag{2.2}$$

where k is the power root index, p_i is the i-th prime number, and I is the number of prime numbers.

The function $f_k(p_i)$ is almost uniformly distributed over the normalized frequency (0,1) and having a dispoint set of irrational numbers. Figure 2.1 is a scatter diagram of the APFF distribution, showing almost uniform distribution, where $k = 2$ and the $I = 10^5$.

In this chapter, the APFA frequencies are created from APFF by using M-partitions with the same number of subcarriers in an OFDM system. The APFF distribution are equally the M-partitions.

The nearest irrational number of prime number i $(1 \le i \le I)$ to m-th partition can be selected as follows;

$$f_{APFA}(k,m) = f_k(p_i), \tag{2.3}$$

where i is the integer such that $|f_m - f_k(p_i)|$ is a minimal value for $1 \le i \le I$, and f_m is given by $m/M - 0.5/M$, with $m = 1, 2, \cdots I$.

The normalized offset frequency (NOF) $\Delta f(k,m)$ is presented by the almost periodic frequency $f_{APFA}(k,m)$ and f_m (m-th partition) as follows;

$$\Delta f(k,m) = f_m - f_{APFA}(k,m), \tag{2.4}$$

By Weyls uniform distribution theorem, APFF $f_k(p)$ is almost uniformly distributed over the normalized frequency (0,1). Thus, a scatter diagram of the APFF distribution when $k = 2$ is shown in Fig. 2.1.

The normalized standard deviation $\sigma_{k,M}$ of NOF are calculated as follow:

$$\sigma_{k,M} = \sqrt{\frac{\sum_{m=1}^{M} \Delta f(k,m)^2}{M}}. \tag{2.5}$$

Figure 2.2 shows the probability mass function (PMF) of APFF intervals corresponding to scatter diagrams of adjacent APFF with $k = 2$.

Figure 2.3 and Figure 2.5 show a scatter diagram of APFF with k=3 and k=5, respectively. It is observed that the scatter diagram of the APFF distribution are not uniformly distributed compared with the case of k=2. However, in Fig. 2.4 and Fig. 2.6, the PMF of APFF demonstrates that APFF $f_k(p)$ exists concentratedly. Moreover, the same tendency is demonstrated for k=7 or more.

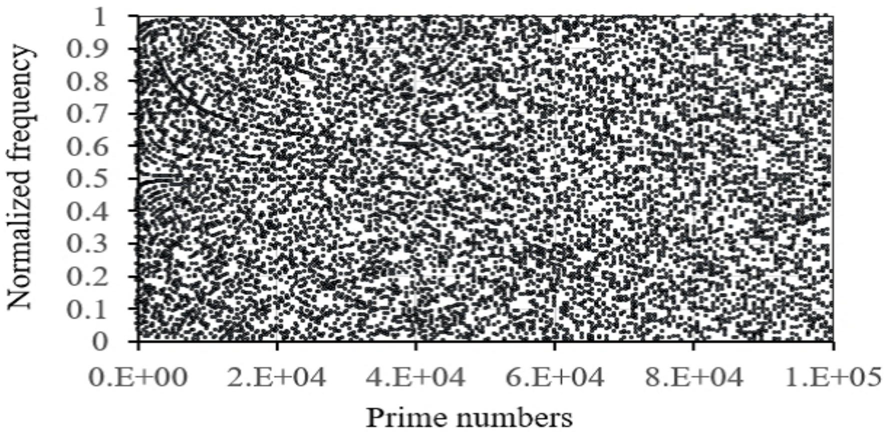

Figure 2.1: Scatter diagram of normalized frequency at *k=2*.

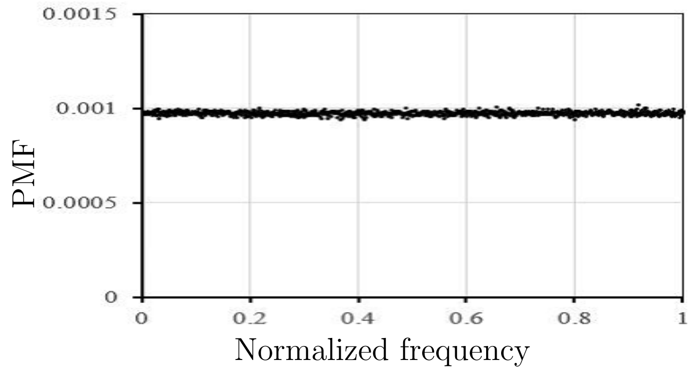

Figure 2.2: Probability mass function at k=2 for prime numbers less than or equal to P_N=5,000,000.

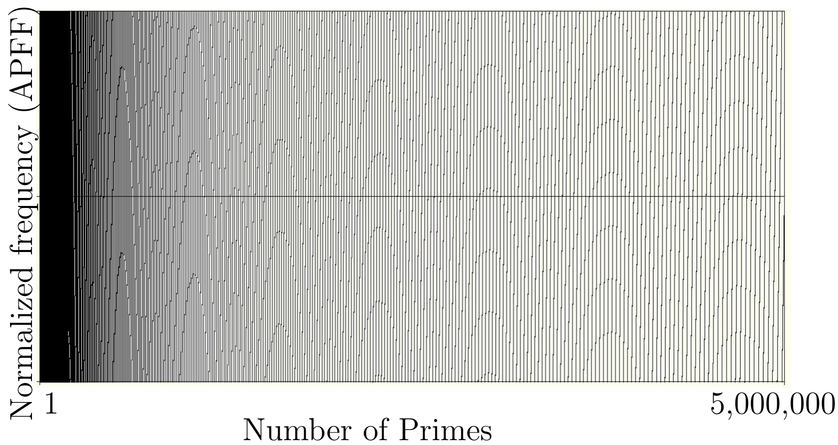

Figure 2.3: Scatter diagram of normalized frequency at k=*3*.

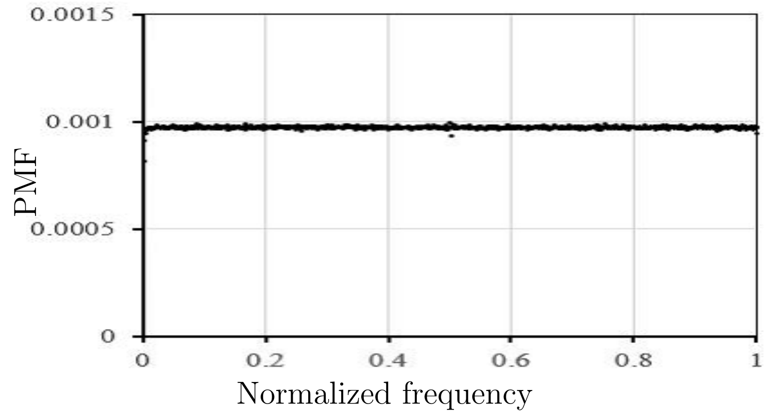

Figure 2.4: Probability mass function at k=3 for prime numbers less than or equal to P_N=5,000,000.

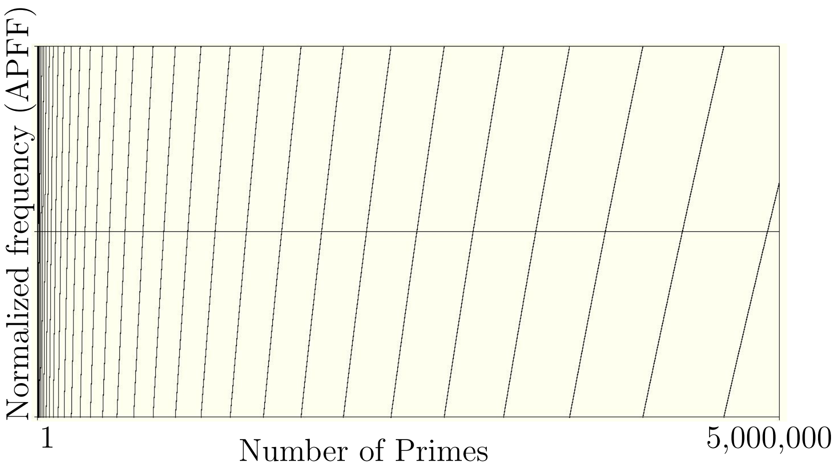

Figure 2.5: Scatter diagram of the normalized frequency at *k=5.*

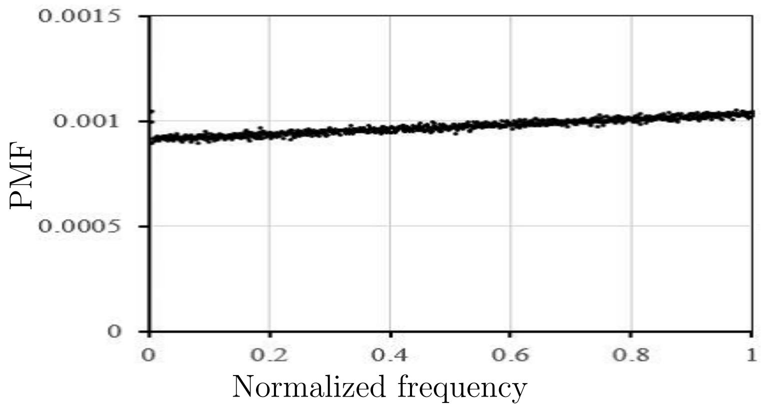

Figure 2.6: Probability mass function at k=5 for prime numbers less than or equal to P_N=5,000,000.

2.2 Uniform distribution

Although there are χ square distribution (chi-square) and F distribution to verify uniform distribution, the monotonic increase entropy method is used, since there are some cases where the distribution shows the bell curve.

The normalized entropy of the phase space is defined by the following equation.

$$Ent(\theta) = \frac{\sum_{p=1}^{P_{max}} \mathrm{prob}(\theta_p) \log_2\{\mathrm{prob}(\theta_p)\}}{\log_2 P_{max}}, \tag{2.6}$$

where, p is an index number of independent variables, P_{max} is the total number of independent variables, and θ_p is the phase of the sampling point.

Normalized entropy approaches unity as the probability density function to be evaluated approaches the uniform distribution. Here, we use complementary normalized entropy (C-Ent) because we want to assess the degree of uniform distribution. The complementary normalized entropy of the phase space is defined by the following equation.

$$\text{C-Ent}(\theta) = \frac{\log_2 P_{max} - \sum_{p=1}^{P_{max}} \mathrm{prob}(\theta_p) \log_2\{\mathrm{prob}(\theta_p)\}}{\log_2 P_{max}}, \tag{2.7}$$

The complementary normalized entropies for the total prime numbers are shown in Fig. 2.7. It can be seen that when the power root is 2 to 3, the complementary normalized entropy is relatively small and uniformly distributed.

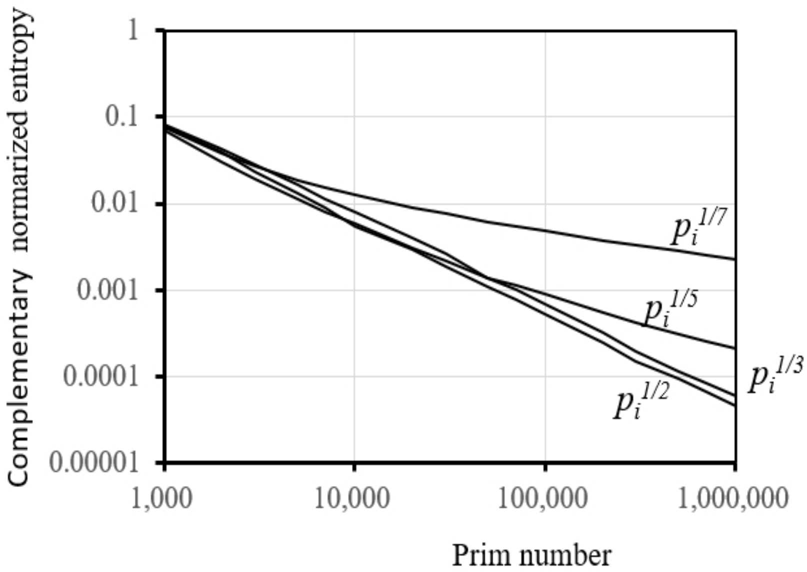

Figure 2.7: Complementary normalized entropies where p_i is i-th prime number.

2.3 APFA Configuration and Features

Figure 2.8 shows the frame structure of OFDM and APFA. The APFA slot frame is the same as OFDM, but instead of the OFDM guard interval, the APFA preparation interval (P in Fig. 2.8) takes 25% of the slot frame for system evaluation.

The frequency of the $m-$th subcarrier of OFDM is demonstrated using the expression as follows.

$$f_m = \frac{1}{M}m - \frac{1}{2M}, \quad (1 \leq m \leq M), \tag{2.8}$$

where, M is the number of subcarriers of OFDM system, m is the m-th subcarrier number.

Using the target frequency (f_m), the normalized offset frequency (NOF after this) of each $f_{APFF}(k, m)$ given by $\Delta f_k(m, P_N)$ is shown in Eq. (2.9).

$f_{APFF}(k, m) = f_k(p)$ where $p \leq P_N$ is the integer such that $|f_k(p) - f_m|$ is a minimal valu for $1 \leq p \leq P_N$.

$$\Delta f_k(m, P_N) = f_m - f_{APFF}(k, m). \tag{2.9}$$

Therefore, the standard deviation $\sigma_M(k, P_N)$ of the $f_{APFF}(k, m)$ can be calculated using the following equation.

$$\sigma_M(k, P_N) = \sqrt{\frac{\sum_{m=1}^{M} \{\Delta f_k(m, P_N)\}^2}{M}}. \tag{2.10}$$

Figure 2.9 shows the target frequency arrangement of the OFDM system having pure carriers, and Fig. 2.10 shows the frequency arrangement of the APFA system with almost periodic frequency width.

Since the arrangement is normalized and distributed on the unit interval (0. 1), when the bandwidth of OFDM or APFA is BW (Hz), the frequency interval f_0, the symbol time length $S(sec)$ are expressed by the equations $f_0 = \frac{1}{M}$ and $S = M$.

Figure 2.11 show the relation between P_N, the number of subcarriers M, and the standard deviation $\sigma_M(k, P_N)$ obtained via using the

APFA scheme. From these data, we obtained a common approximation of standard deviation $\sigma_M(k, P_N)$ of NOF that holds regardless of k from data according to the following expression as shown in Eq. (2.10).

The closeness of the selected almost periodic frequency to the normalized frequency, can be evaluated via the frequency standard deviation σ_M of differences from the target frequency arrangement (TFA).

The APFA proposed here is generated with reference to a target frequency, which can be arranged at arbitrary intervals of a normalized frequency range (FR) being greater than 0, and less than 1, and by selecting the subcarrier frequency APFF close to the k-th root of the target number of prime numbers.

The procedure for determining the M and σ_M of APFA is as follows.

Step1. Determine the number of subcarriers M. The communication capacity of the system is determined by the transmission rate and the number of subcarriers M.

Step 2. Determine the σ_M of differences from the TFA. The closeness of the selected almost periodic frequency to the TFA means that the peak-to-average power ratio (PAPR) is near to the PAPR of OFDM as σ_M decreases. Therefore, the σ_M of APFA is determined from the PAPR design target.

Step 3. The prime number P_N and k for obtaining the k-th root are determined from Eq. (2.11).

Eq. (2.11) is obtained by regression analysis of a curve representing the relationship between $\sigma_M(k, P_N)$, and P_N in Fig. 2.11. When the number of subcarriers is determined, the number of primes P_N is calculated to obtain the target standard deviation $\sigma_M(k, P_N)$ by using Eq. (2.11).

Figure 2.11 and Eq. (2.11) correspond to up to two million subcarriers, so we have obtained a relational expression that enables APFA frequency allocation with greater than one million subcarriers.

$$\sigma_M(k, P_N) = 10^{-0.164335-0.997811\times(\log_{10} M-\log_{10} P_N)}(2 \leq M \leq 2,097,152). \tag{2.11}$$

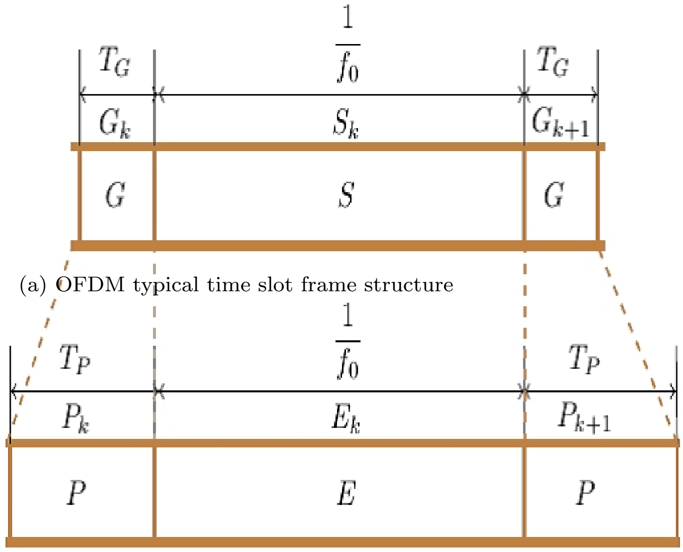

(a) OFDM typical time slot frame structure

(b) APFA time slot frame structure

Figure 2.8: Time slot frame structure for evaluation simulation,
S: symbol interval,
G: guard interval,
S_k: k-th symbol,
G_k: k-th guard,
T_G: Time guard interval,
E: evaluation symbol interval,
P: preparation interval,
E_k: k-th evaluation symbol,
P_k: k-th preparation signal,
f_0: Frequency interval of subcarrier,
P_E: Time length of evaluation interval,
f_0:Frequency interval of the subcarriers.

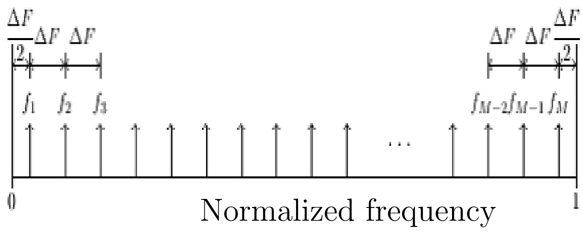

Figure 2.9: OFDM frequency arrangement(0-1).

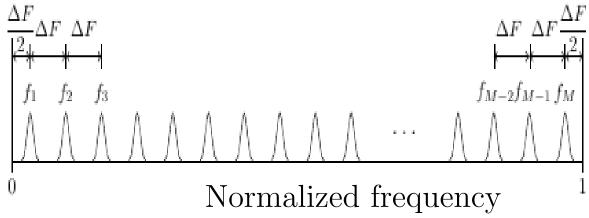

Figure 2.10: APFA of frame structure (0-1)

APFA of frame structure (0-1) $\Delta F = f_0 : Frequency\ interval\ of\ subcarrier.$

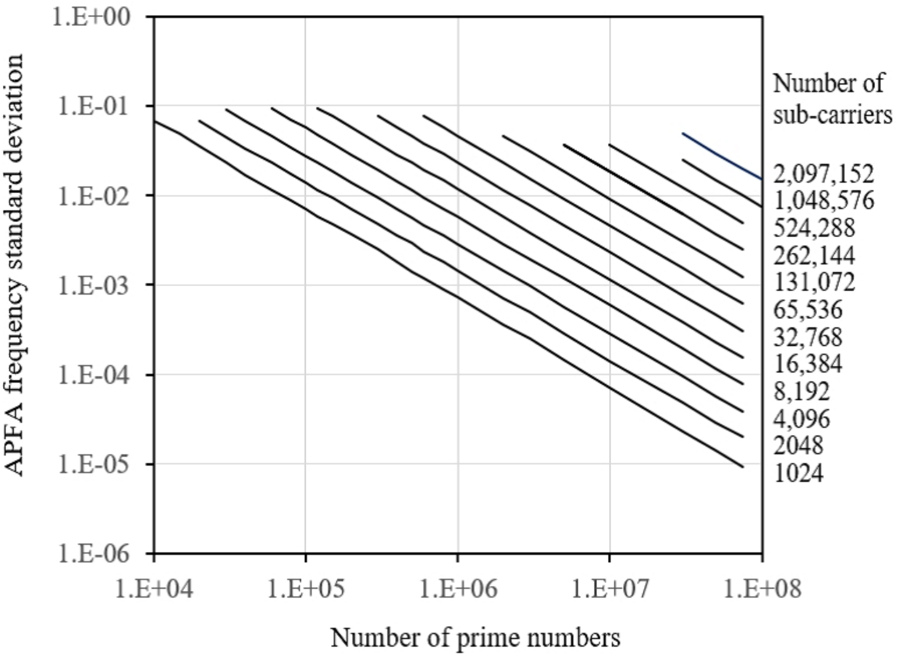

Figure 2.11: NOF standard deviation $\sigma_M(k, P_N)$ with respect to the number of primes
(the number of subcarriers: $1024 \sim 2,097,152$ channels).

2.4 Inter-Symbol Interference

In frequency-division multiplexing transmission, inter-carrier interference (ICI) increases by the transmitting power amplifier nonlinearity. The input output characteristics of an power amplifier having nonlinear characteristics are generally expressed as follows.

$$y(t) = a_1 \sum_{m=1}^{M} x_m(t) + a_3 \left[\sum_{m=1}^{M} x_m(t)\right]^3 + a_5 \left[\sum_{m=1}^{M} x_m(t)\right]^5 + a_7 \left[\sum_{m=1}^{M} x_m(t)\right]^7 + \cdots, \quad (2.12)$$

where, a_n: n-th coefficient of the input and output characteristics, m: the subcarrier index number of frequency-division multiplexing transmission.

When multiple signals are superimposed, the mutual modulation product by the third strain is expressed by the following expression using the polynomial theorem.

$$\left[\sum_{m=1}^{M} x_m(t)\right]^3 = \frac{3!}{q_1!\, q_2! \cdots q_m!} x_1^{q_1} x_2^{q_2} \cdots x_m^{q_m}, \quad (2.13)$$

where $q_1, q_2, \cdots, q_m \geq 0$, and $q_1 + q_2 + \cdots + q_m$=3.

In OFDM system, three waves x_{m-1}, x_m, and x_{m+1} are expressed by the frequency component orthogonal to the rational number, and the intermodulation product is expressed as an integral multiple of the frequencies of three waves. This means that the intermodulation product wave matches any of the subcarriers of the transmitted signal because all the subcarrier spacings are the same. In the APFA system, this means that the intermodulation product does not match any of the subcarriers of the transmitted signal.

In order to investigate the influence of the nonlinearity of the amplifier for the frequency division multiplexed signals, the level fluctuation of the subcarrier and the spectrum of ICI between the subcarriers were examined by computer simulation. Figure 2.12 shows a standard deviation of the level fluctuation of subcarriers of the OFDM and the APFA. If the input level is close to the saturation level of the amplifier, the standard deviation of each subcarrier level of OFDM is slightly larger than APFA.

Figure 2.13 shows the spectrum distribution around subcarriers, OFDM indicates that less spread spectrum components compared to APFA. That is, in the nonlinear effects of the amplifier, the effect of APFA spreads the spectrum around the subcarrier, and the near subcarrier are influenced with the power sum, and the OFDM with the voltage sum.
There, APFA has less system impact on nonlinear interference than the OFDM.

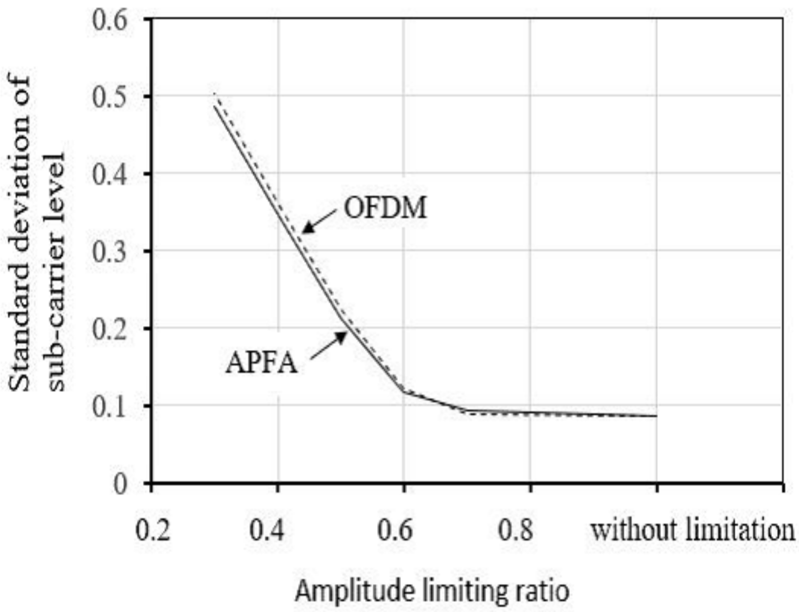

Figure 2.12: Standard deviation of a subcarrier level for amplitude limiting ratio with the normalized value of the power being 0.35.

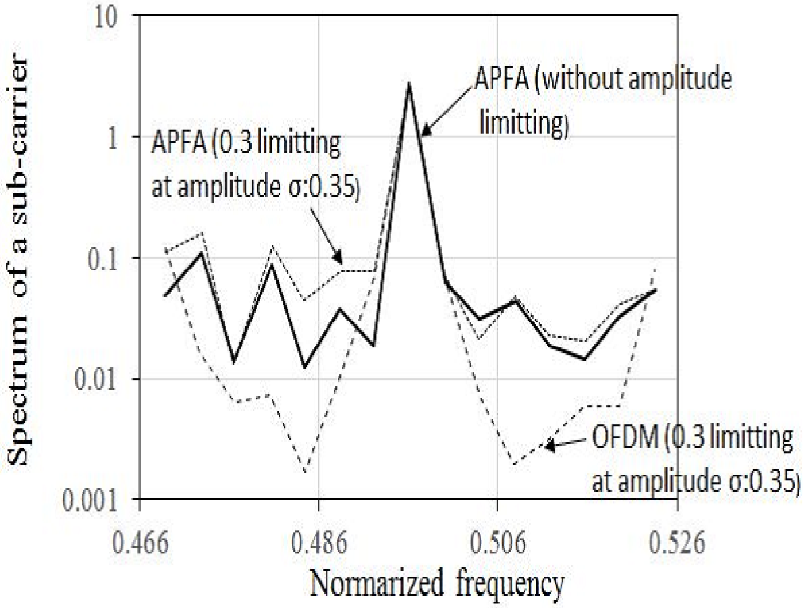

Figure 2.13: Spectrum distribution around the subcarriers for amplitude limiting ratio with the normalized value of the power being 0.35.

2.5 Evaluation Procedure

2.5.1 Computer Simulation Configuration

Functional composition of simulation is for verifying the communication performance of APFA system, and we previously reported that it was configured to be able to perform system evaluation of transmission and receiver characteristics for APFA [12]. The transmitting side has an APFA frequency generation and code modulation function, combining and transmitting functions of APFA, and the receiving side has a decoding function by complex correlation, an error rate measuring function, and PAPR evaluation block to compare with OFDM communication.

The computer simulation of the APFA has the ability to simulate prime numbers up to *one millions* , so that it can evaluate the supermultiplexing [14][15].

The computer simulation for the performance evaluation used by this research is shown and the list in Fig. 2.14 of the function is shown in Table 2.1. The computer simulation has evaluation functions of the chaos code and general code. While this diagram is a computer simulation of the APFA, it is also compatible with the constant power chaos spreading code, so that it can evaluate the chaos code and more general codes, too. The computer simulation of the APFA has also the ability to simulate prime numbers up to 100 million, so that it can evaluate the super-multiplexing, too, which is one of the main research topics. Moreover, it observes imbalances of the subcarrier numbers and imbalance of the modulation code to prevent the setting failure.

The computer simulation diagram for the performance evaluation used in this research is shown in Fig. 2.14 and the list of the basic functions is shown in Table 2.1.

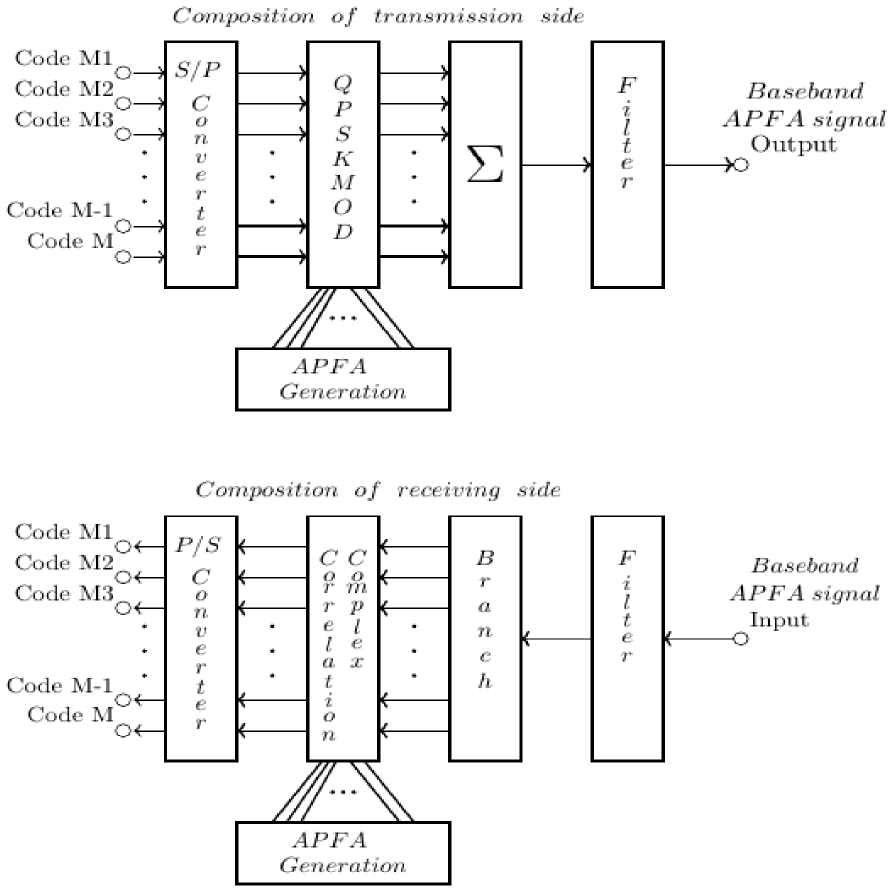

Figure 2.14: Functional composition of simulation for characterization.

The frequency use efficiency can be secured for three types of chaotic codes by using usual cosine roll-off filters as Fig. 2.15. We use the rectangular filter from the spectrums shown in uniformity of APFA sequences as shown in Fig. 2.16.

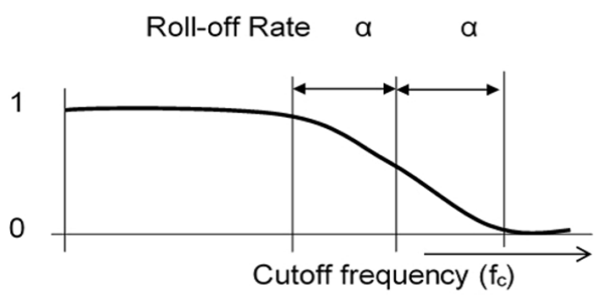

Figure 2.15: Cosine roll-off filters characteristic.

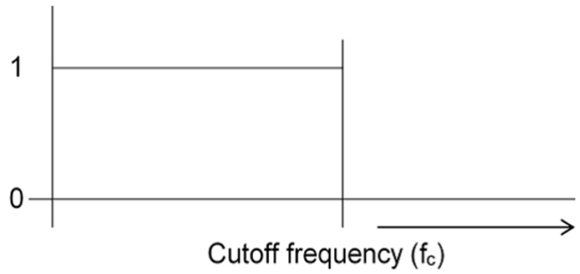

Figure 2.16: Rectangular filter characteristic.

Table 2.1: Composition and list of functions of the evaluation computer simulation.

Functional block	Content of function
Calculation of prime number	Prime number within one billion
Modulation function	QPSK modulation
Sign generator capability	M sequence code generation, or Walsh code, or Pseudo-random
APFA transform operation facility	Subcarrier sum with over samplings ≤ 32
Noise generation function	Generation of AWGN signal
APFA receiving operation facility	Complex cross-correlation with over samplings ≤ 32
Evaluation function	PAPR of transmitting signa, Probability density distribution of amplitude, Cumulative distribution of amplitude,Complex auto-correlation, Primitive root sign generation, Square solvable function
Function for evaluation of encoding by almost periodic function	Phase entropy evaluation, Phase probability density distribution, Phase standard deviation

2.5.2 Transmission Signal and Receive Signal Processing

The transmission signal is expressed by the following Eq. (2.14) where each approximately periodic frequency components of APFA are modulated by QAM (Quadrature Amplitude Modulation).

$$TX(t) = \sum_{m=1}^{M} Code_m \times e^{j2\pi f_{APFA}(k,m)t + j\theta_m}, \tag{2.14}$$

where M is the number of subcarriers of APFA system, m is the m-th subcarrier number, $Code_m$ is the modulation code of m-th subcarrier, and θ_m is a phase (radian) of m-th subcarrier.

In multicarrier communication schemes such as APFA, an exceedingly large peak of signals is inevitably generated by a combination of codes to be transmitted. The subcarrier is degraded by the transmitting amplifiers saturation. The transmission signal $TX'(t)$ at output of the transmitter is then given by Eq. (2.15), where s is the ratio of the saturation level and the standard deviation σ_τ of transmission signal $TX(t)$.

$$TX'(t) = \begin{cases} \sum_{m=1}^{M} Code_m \times e^{j2\pi f_{APFA}(k,m)t + j\theta_m}, & \text{if TX(t)} \leq s\sigma_\tau, \\ s\sigma_\tau \times e^{j\theta(t)}, & \text{if TX(t)} > s\sigma_\tau, \end{cases}, \tag{2.15}$$

where, $\theta(t)$ in Eq. (2.15) is given as follows.

$$\theta(t) = \arctan\left[\frac{\sum_{m=1}^{M} Code_m \times \sin\{2\pi f_{APFA}(k,m)t + \theta_m\}}{\sum_{m=1}^{M} Code_m \times \cos\{2\pi f_{APFA}(k,m)t + \theta_m\}}\right]. \tag{2.16}$$

There, $Code_m$ is a modulation code and θ_m is a phase shift for user m due to asynchronism of the APFA system.

Here, the symbol OIP3, OIP5 denotes the following meanings:

OIP3 : 3rd-order output intercept point,

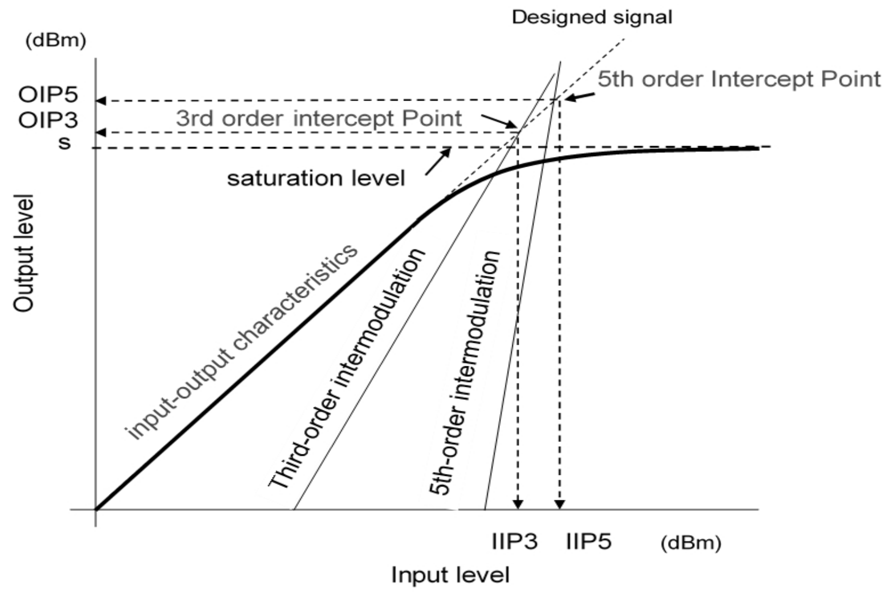

Figure 2.17: Input output characteristics of amplifier.

OIP5 : 5-th-order output intercept point.

The receiving signal is expressed by the Eq. (2.17) where each approximately periodic frequency components of APFA are modulated by QAM (Quadrature Amplitude Modulation) at the transmission side. Since APFA is a quasi-synchronous system, the normal decoding method by FFT used in a synchronous system can not be applied directly. Thus, the complex correlation is accordingly employed to decode a modulation code at the transmission side..

For decoding, we use the same APFF as the transmission system and detect the code on transmitting side from the complex cross correlation ρ with the receiving signal $R_x(t)$ and reference signal $S_m(t)$ as shown in Eq. (2.18).

$$R_x(t) = \sum_{m=1}^{M} \dot{I_m} \times Code_m \times e^{j2\pi f_{APFA}(k,m)t + j\theta_m} + \mathbf{N} + \mathbf{I}, \qquad (2.17)$$

where, $\dot{I_m}$ is a transmission characteristic expressed by a complex number, $\mathbf{N}$ are noises generated in the propagation path, and $\mathbf{I}$ are interference radio waves generated in the propagation path.

$$\rho(R_x, {S^*}_m) = \frac{\frac{1}{T_m}\int_0^{T_m}(R_x(t), {S^*}_m)dt}{\frac{1}{T_m} \times \sqrt{\int_0^{T_m}(R_x(t), {R^*}_x(t))dt} \times \sqrt{\int_0^{T_m}(S_m(t), {S^*}_m(t))dt}}, \tag{2.18}$$

where, $S_m(t) = e^{j2\pi\times \mathrm{f_{APFA}(k,m)\times t}}$, $T_m = \lceil M \times f_{APFA}(k,m) \rceil / f_{APFA}(k,m)$, $\lceil \ \rceil$ means a ceiling function, and $*$ means complex conjugate.

Figure 2.17 shows typical input-output characteristics of the amplifier, and illustrates a third-order intercept point (IIP3), a 5-th order intercept point (IIP5), and a saturation level s .The 3rd order intercept point (IIP3) corresponds to the 3rd order distortion, and the 5-th order intercept point (IIP5) corresponds to the 5-th order distortion. The saturation level s is the maximum output power of the amplifier, and the transmission power is limited to this level.

Figure 2.18 shows asynchronous phase diagram of APFA transmission signal of the subcarrier frequency configuration when the performance of the transmission amplifier (Fig. 2.17) is expressed by the hard limiter (Fig. 2.18-b,c) or without the transmission amplifier (Fig. 2.18-a).

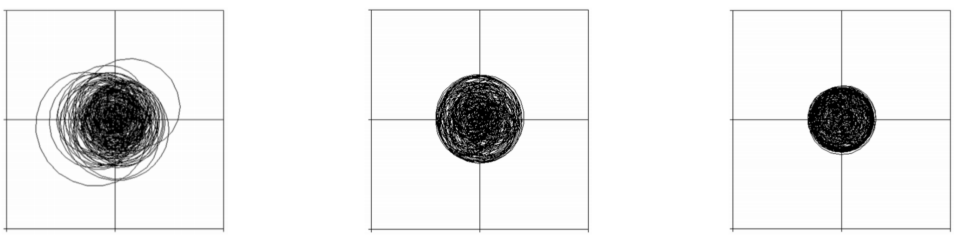

(a) Saturation level : linear

(b) Saturation level :1.5 σ_τ

(c) Saturation level : 1.1 σ_τ

Figure 2.18: Asynchronous constellation diagram of the transmission signal of subcarrier frequency configuration in case of k=3.

2.6 PAPR and Compensation

A synthetic wave at an exceedingly high level has been suppressed to a certain degree by the saturation property of the power amplifier of the final stage of the transmitting side. However, the PAPR suppression owing to the saturation property also exhibits the same problems, which increases the effective bandwidth and channel interference between the subcarriers. In this section, the degradation of the PAPR and interchannel interferences are evaluated using a bandlimited peak complex suppression method. The transmitting power of the satellite communication is affected by the efficiency of the power amplifier in the transmitter and PAPR of the transmission signal. PAPR is usually defined via the following expressions:

$$PAPR = 10 \times \log_{10} \frac{max[(x(t)x^*(t)]}{E[x(t)x^*(t)]}, \quad [dB], \tag{2.19}$$

where, x(t) is a transmission signal and E$[x(t)x^*(t)]$ refers to the square mean value.

There is a problem where a high peak level is generated in the transmission signal in the case of OFDM modulation system and the research to decrease PAPR is continued. Degradation of PAPR along with super-multiplexing is already proven [14]. Therefore, the development of the PAPR compensation technology is required while suppressing the interference between the subcarrier and the bandwidth that refers to the width of pass band. We propose the PAPR compensation scheme (peak value complex suppressive method) that can correspond to supermultiplexing without depending on the number of subcarriers of the synthetic signal. Compensation signals are defined using the following expressions:

$$z_0(i) = z_(i) - \sum_{l} \sum_{-t}^{t} \Delta A \times h(t, l), \tag{2.20}$$

where $z_i(i)$ is the i-th complex input signal, $z_o(i)$ is the i-th complex output signal, ΔA is the peak level (regulated value) and $h(t, l)$ is an l-th finite impulse on time t.

2.7 Characteristics Related to Radio Communication

Figure 2.19 shows the PAPR value to the normalized frequency deviation of NOF with the peak limitation level as a parameter when the number of subcarriers equals 256. The frequency standard deflection of the abscissa demonstrates the amount of the normalized frequency deviation of NOF. Further, this means that APFA is close to the OFDM frequency allocation as the frequency standard deviation σ_M of NOF is smaller. If there is no compensation of PAPR such that σ_M is less than or equal 0.07 in Fig. 2.19. In this case, the PAPR is near the normal PAPR of OFDM which is approximately 10 dB. The PAPR is near arround a constant value with respect to σ_M with the compensation method in Fig. 2.19.

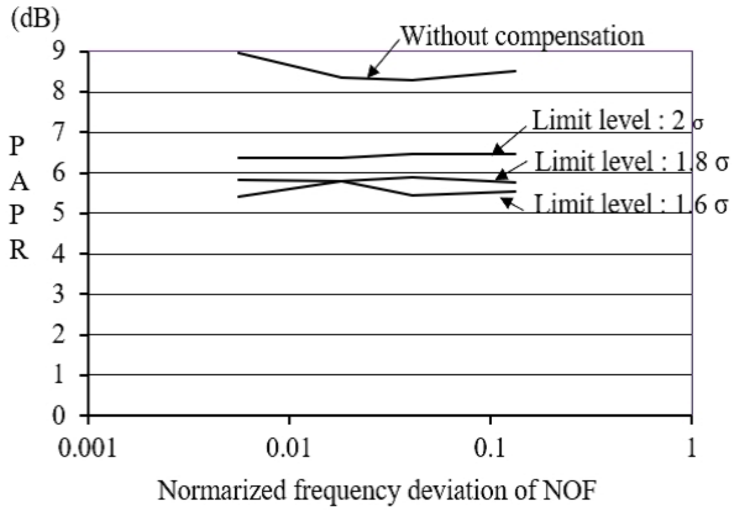

Figure 2.19: Normalized frequency deviation vs. PAPR.

2.8 Modulation Error Ratio (MER) Characteristic

MER is used to show the modulation quality of the level of the digital modulation signal and the phase quantitatively, and it is expressed by the vector synthesis of constellation of the modulation wave shown in Fig. 2.20 and the signal error vector. MER is defined by Eq. (2.21).

MER shows a value of about 30 dB in Fig. 2.21 between the number of the subcarriers is from 32 to 16,000 with the frequency standard deviation σ of the NOF being at about 0.09. This indicates that the stable MER value is shown if $\sigma_{k,M}$ is the same even if the number of subcarriers is increased.

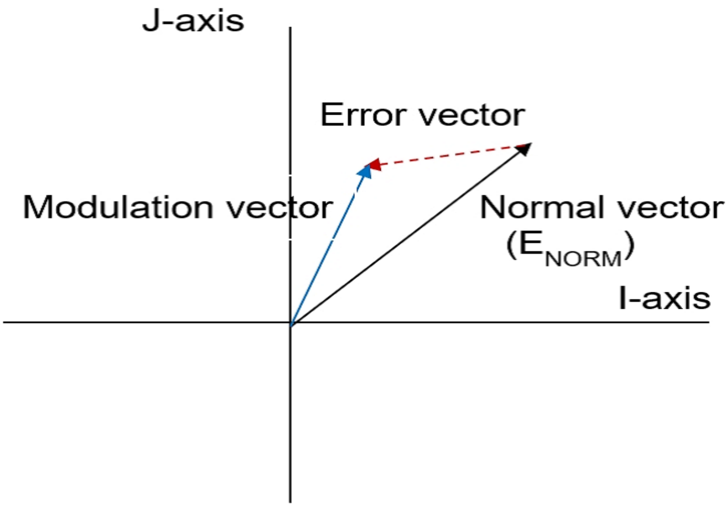

Figure 2.20: Image of modulation vector in which deterioration is received
($|E_{NORM}|$: The normalized value of the n-th normal vector).

$$MER \equiv 10 \log \frac{\sum_{n=1}^{N} \left(\overline{E}_I^2 + \overline{E}_J^2 \right)}{\sum_{n=1}^{N} \left((E_I - \overline{E}_I)^2 + (E_J - \overline{E}_J)^2 \right)}, \tag{2.21}$$

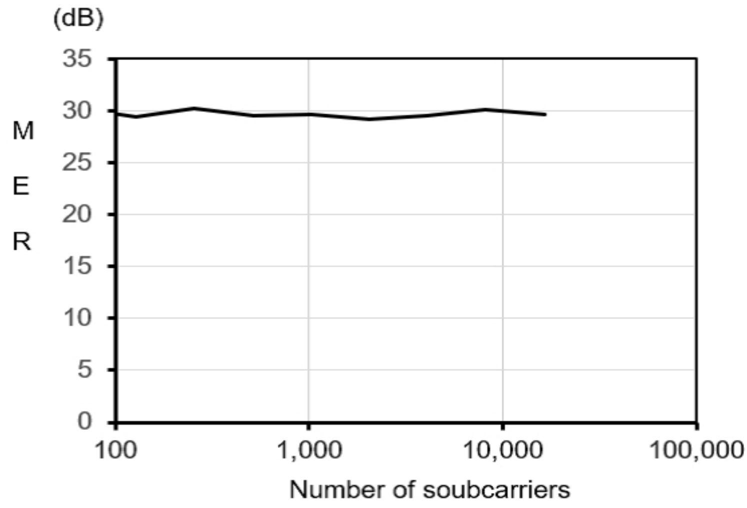

Figure 2.21: Total number of subcarrier numbers vs. MER characteristic.

where, E_I is the n-th in-phase component of the modulated signal, E_J is the n-th quadrature component of the modulated signal, $\overline{E}_I$ is the n-th in-phase component of regular vector, and $\overline{E}_J$ is n-th quadrature component of regular vector.

2.9 Bit Error Rate (BER) Characteristic

Figures 2.22, 2.23 show the various simulation results of BER performance of the APFA system for E_b/N_0 (signal energy per symbol to noise power ratio) obtained by varing σ in case of QPSK modulation method.

When the condition of σ_M is small, the BER characteristic indicates a value close to the theoretical value. However the condition of σ_M is over 0.05, there are a little error floor in the BER characteristics at $E_b/N_0 = 7dB$ as shown in Fig. 2.22. This is due to the asynchronous nature of APFA. Theoretical BER characteristics of QPSK modulation method in Figs. 2.22, 2.23 are values calculated from an error function given by Eq. (2.22) [42]. Figure 2.24 shows the BER characteristic with respect to the number of subcarriers at $\sigma_{k,M}$ of NOF = 0.013. The BER characteristic shows a value close to the theoretical value even if the number of subcarriers changes from 1,024 to 524,288 channels. This indicates that it does not affect the frequency multiplexing of the APFA.

$$BER = \frac{1}{2} \times erfc\left(\frac{E_b}{N_0}\right), \tag{2.22}$$

where erfc(x) is the error function defined as follows:

$$erfc(x) = \frac{2}{\sqrt{\pi}} \times \int_x^\infty e^{-t^2}\, dt. \tag{2.23}$$

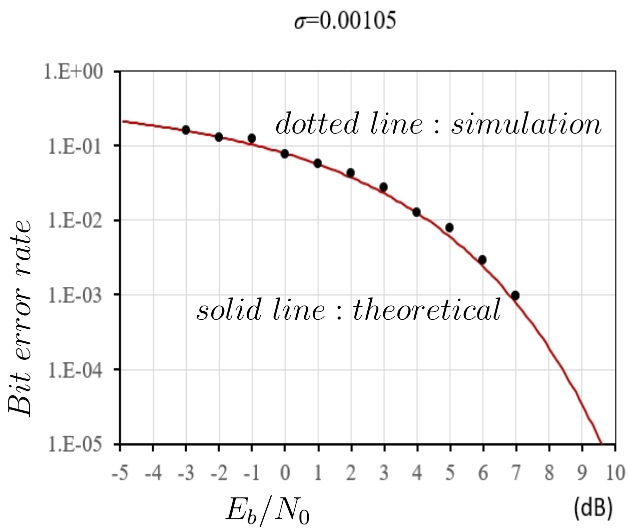

Figure 2.22: BER performance of APFA system with $\sigma_{k,M}$ being NOF is 0.00105.

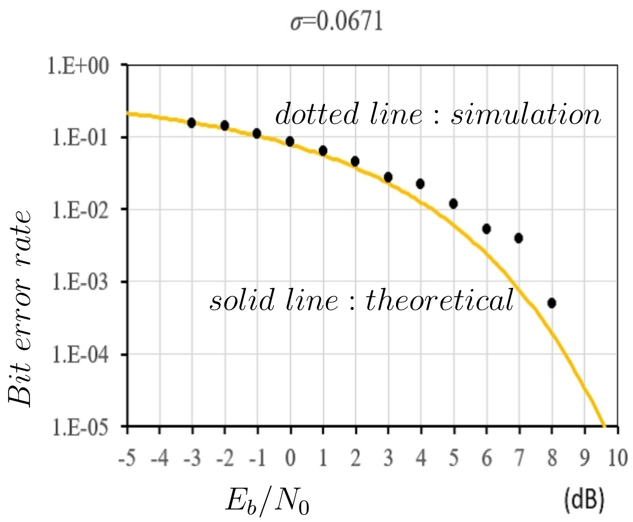

Figure 2.23: BER Performance of APFA system with $\sigma_{k,M}$ of NOF being 0.0671.

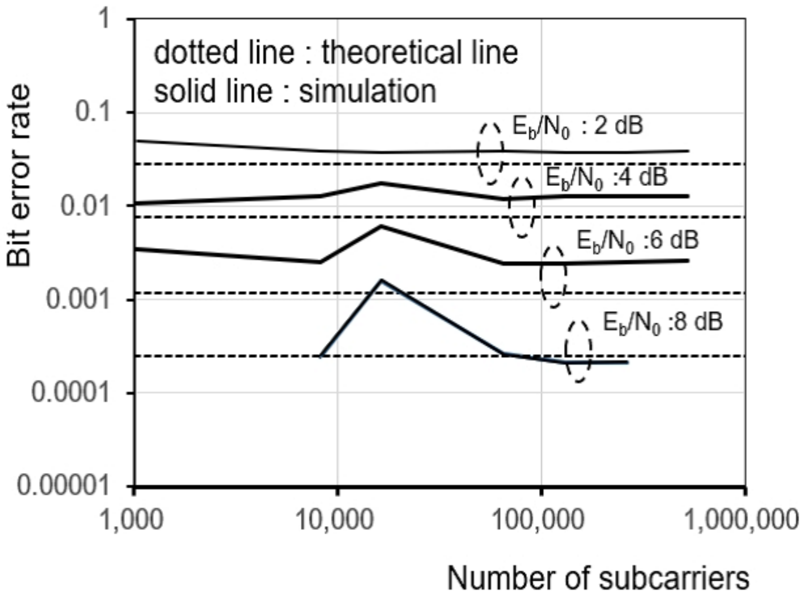

Figure 2.24: The total number of subcarriers for 1024 to 524,288 channels vs. BER characteristic where $\sigma_{k,M}$ of NOF is 0.013.

2.10 Conclusions

We propose at new concept of communication methods, that is the wireless communication systems based on the disjoint sets of irrational numbers for frequency allocation which are completely different from the existing communication systems that use the rational numbers to specify frequency.

Although APFA is the system of asynchronous communication, we have shown that the BER characteristic exhibits a value similar to the theoretical value by performing complex valued synchronization detection. The BER characteristic shows a value close to the theoretical value even when the number of channels changes. This indicates that it does not affect the frequency multiplexing capability of the APFA as shown in Fig. 2.24

In this chapter, we propese the normalized entropy method of the phase space for the uniform distribution and the complementary normalized entropy method (C-Ent) of the phase space for the high-level uniform distribution.

We also propose a PAPR compensation method to reduce the PAPR on the APFA transmitting signal. In Fig. 2.19, the PAPR without compensation is approximately 9 dB, while PAPR can be improved to be approximately 6 dB with compensation.

Chapter 3

APFA systems

In Chapter 3, we describe the basic principle of the sub-carriers of APFA using disjoint sets of irrational numbers and APFA having the spectrum characteristic of normalized offset frequency (NOF).

3.1 Basic Principle

The subcarrier frequency of the existing OFDM system or OFDMA system needs to be composed of rational number groups, while the APFA system has an *almost periodic frequency arrangement* with respect to the combination of disjoint sets of irrational number groups for the dispersion of coupled waves due to the nonlinear distortion of devices.

In order to select subcarrier frequencies M channels of APFA out of the disjoint irrational number groups, the Dedekind cuts were used to put rational number partitions into irrational numbers [10][11]. These Dedekind cuts show that there are irrational numbers within rational number partitions.

The APFA scheme is using the signal of L_2 space.

3.2 Subcarrier Frequency of APFA

We define APFF (almost periodic functions frequencies) which transform by linear mapping of the disjoint sets irrational number groups IG(u) as follows;

$$f_d(u) \equiv IG(u) \ (\ \mathrm{mod}\ 1\ ), \quad u = \mathit{1}, \mathit{2}, \cdots U, \tag{3.1}$$

where u is the serial number of disjoint sets of irrational number groups and U is the number of irrational group.

The APFF $f_d(u)$ is almost uniformly distributed over the normalized frequency (0,1) and have a disjoint sets of irrational numbers.

The APFA frequencies are created from APFF by using M-partitions with the same number of subcarriers in an OFDM system. When the number of irrational group U is sufficiently large, the APFF frequency probability distribution between M-partitions is uniformly distributed and is expressed as the uniform distribution as $p(u)$=$\frac{1}{U}$, $u = 1, 2, \cdots U$.

The nearest irrational number of prime number for $1 \leq u \leq U$ to m-th partition can be selected as follows;

$$f_{APFA}(m) \ = f_d(u), \tag{3.2}$$

where u is the integer such that $|f_d(u) - f_m|$ is the minimal value for $1 \leq u \leq U$, and f_m is given by $m\Delta F - 0.5\Delta F$ with m=1,2,$\cdots M$.

The normalized offset frequency (NOF) $\Delta f_d(u)$ is presented by the almost periodic frequency $f_{APFA}(u)$ and f_m (m-th partition) as follows;

$$\Delta f_d(m) = f_{APFA}(m) - f_m,\ m = 1, 2, \cdots M. \tag{3.3}$$

The normalized standard deviation $\sigma_d(M)$ of NOF are then calculated by the follows;

$$\sigma_d(M) = \sqrt{\frac{\sum_{m=1}^{M} \Delta f_d(m)^2}{M}}. \tag{3.4}$$

When the disjoint sets of irrational numbers is a power root of the prime number, the following relationships are held from equations in section 2.3.

$$\Delta f(k, m) \equiv \Delta f_d(m) \tag{3.5}$$

$$\sigma_M(k, P_N) \equiv \sigma_d(M) \tag{3.6}$$

3.3 APFA Characteristics on Base band Frequency Arrangement

Since the power root of a prime number is an irrational number, the APFF frequency can be configured with an irrational number.

Figure 3.1 shows an example of the frequency arrangement of OFDM, where $\Delta F = 1/M$.

Figure 3.2 shows an example of the frequency arrangement of APFA. The center frequency of the APFA subcarriers corresponds to the separation made by the rational number of the irrational frequency group, and it is the same as the OFDM system or the OFDMA system as depicted in Fig. 3.1.

The APFA subcarriers are distributed around the center frequency by the normalized standard deviation $\sigma_M(k, P_N)$ from the center frequency f_m which is the same as the main OFDM system or the OFDMA system in Eq. (3.4) and Eq. (3.6).

In the APFA system, the main signal processing is performed on the base band signal processing. The frequency allocation f_{APFA} on the transmission band is frequency-shifted to the basic frequency allocation F_{APFA} for the positive side by $\Delta F/2$ as

$$F_{APFA}(k,m) \equiv f_{APFA}(k,m) + \frac{\Delta F}{2},\ m = 1, 2 \cdots M. \tag{3.7}$$

The standard deviation $\sigma_M k, \pi(N_a)$ of the NOF can be obtained from Eq. (3.8) given the number of the natural numbers and the number of subcarreis [14]. After using Eq. (3.6), to determine $\sigma_{k,M}$ and the number of subcarriers, the maximum number N_a of the natural numbers to be prepared for the simulation is then obtained.

$$\sigma_{k,M}(\pi(N_a)) = 10^{-0.9719\log_{10}(\pi(N_a)\cdot 64/M)+1.635}, \tag{3.8}$$

where $\pi(N_a)$ is the number of prime numbers in the set of natural numbers less than or equal to N_a.

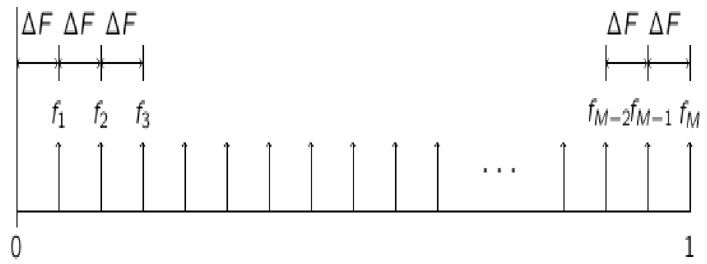

Figure 3.1: Frequency arrangement of OFDM system.

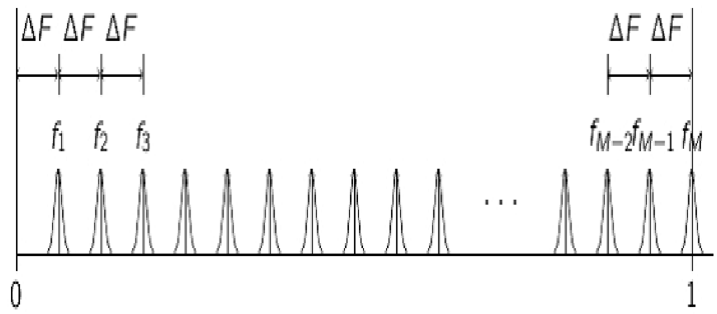

Figure 3.2: Frequency arrangement of APFA system.

3.4 Spectrum Characteristic of Normalized Offset Frequency (NOF)

Since the frequency arrangement is normalized and distributed on the unit interval (0. 1), when the bandwidth of OFDM or APFA is BW (Hz), the frequency interval f_0, and the symbol time length $S(sec)$ are expressed by the equations $f_0 = \frac{1}{M}$ and $S = M$ respectively.

Figures 3.3 to 3.6 show the change in probability mass function (PMF) of the APFA normalized frequency deviation with σ. We found that there are three areas of power spectrum density PSD(f)= $1/f^A$ found in the noise field as follows[16].

Flat area:$PSD(f)$ = constant (white noise)
A=1 area:$PSD(f)$ =$1/f$ (pink noise)
A=2 area:$PSD(f)$ =$1/f^2$ (Brownian noise)

Thus, it can be said that the APFA system contains a flat area (white noise), $1/f$ area, and $1/f^2$ area (Brownian motion noise), as shown indicated in Figs. 3.3 to 3.6.

Figure 3.6 shows the relationship between the standard deviation of the normalized offset frequency (NOF) and the index A of $1/f^A$ with 128 to 1,048,576 subcarriers.

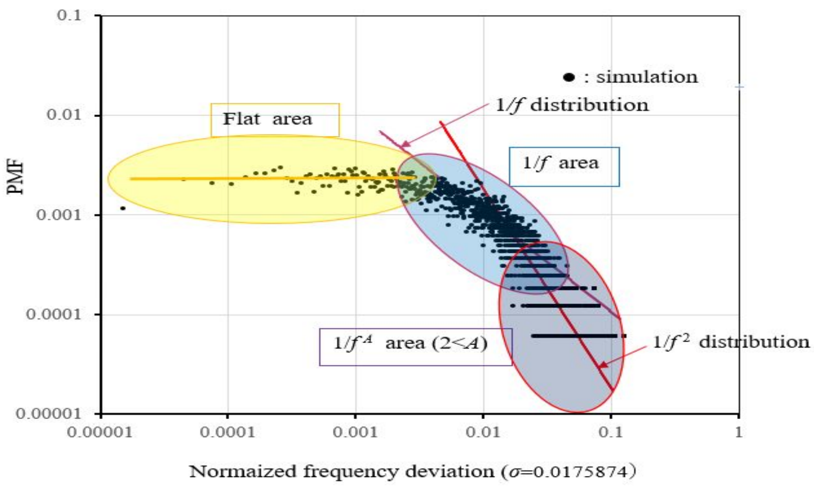

Figure 3.3: NOF of APFA vs. PMF with σ=0.017 where the number of subcarriers is 16,384.

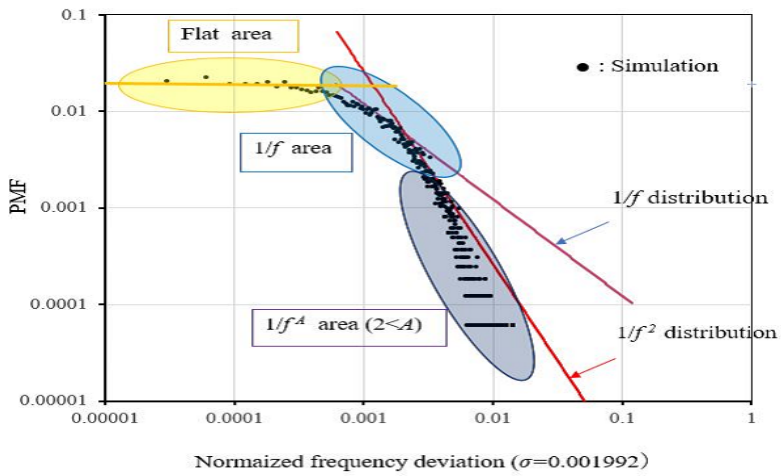

Figure 3.4: NOF of APFA vs. PMF with σ=0.00199 where the number of subcarriers is 16,384.

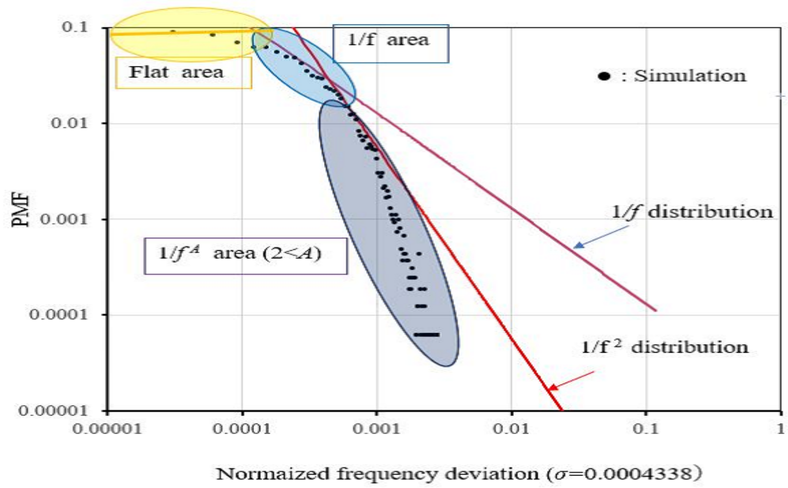

Figure 3.5: NOF of APFA vs. PMF with σ=0.000434 where the number of subcarriers is 16,384.

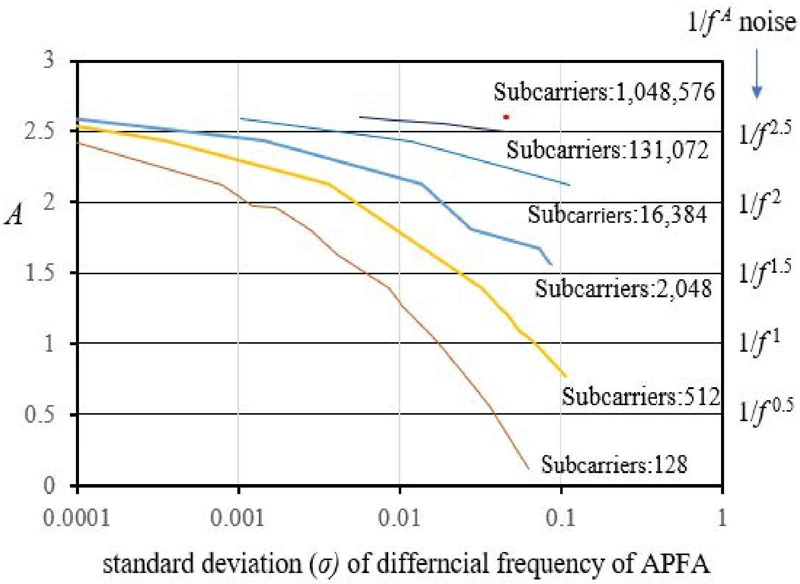

Figure 3.6: The standard deviation of NOF vs. the power index A of $1/f^A$ compared to the number of 1,024 to 1,048,576 subcarriers.

3.5 Conclusions

In Chapter 3, we also show new concept of APFA that enables subcarrier f and ultrawide band communications of up to one million channels and the basic performance using computer simulations. We found that probability mass function PMF of the APFA has three areas of power spectrum density (PSD(f)= $1/f^A$) found in the noise field [14] as shown in Figs. 3.3 to 3.5.

Flat area:$PSD(f)$ = constant (white noise)
A=1 area:$PSD(f)$ =$1/f$ (pink noise)
A=2 area:$PSD(f)$ =$1/f^2$ (Brownian noise)

The relationship between the power A of PSD(f)= $1/f^A$ and chaotic feature is considered as a future research theme.

Chapter 4

Chaotic Property of APFA

In this chapter, we propose a new frame Lyapunov exponent (FLE)[17] which can estimate the phase difference sensitivity depending on the frame number and reveal the universal feature of FLE and elucidate several characteristics such as short-term radiations of phases. We propose chaos-APFA method to aim the optical communication system or THz radio communication system by the 2D exactly solvable chaos code .

4.1 Frame Lyapunov Exponent (FLE)

Recently, chaotic spreading codes generated by almost periodic functions where reported to be advantageous for super-multi access communications. Additionally, simulation results for applicability to satellite communications are reported, and it has been observed that almost periodic frequency arrangement (APFA) has a different characteristics as compared to that of existing periodic signals.

That means that the higher the number of subcarriers and the frequency division are the more necessary it is to construct communication systems such as APFA system corresponding to the frequency division multiplexing frequency.

We already reported that it has an ability to connect more than one million terminals at a base station by using the super-multicarrier APFA signal modulation scheme.

The APFA scheme is an asynchronous multi-carrier frequency arrangement with quasi-orthogonality. In this chapter. we introduce the new frame Lyapunov exponent which can estimate the phase difference sensitivity of APFA systems.

In the elucidation of frame Lyapunov exponent (FLE) $\lambda(n)$ in double logarithm, Q_1 means the primary component (slope) of initial sensitivity, C_0 and $C(n)$ refer to the stationary long-term and the short-term variation of FLE in which n is the number of frame numbers respectively.

$f_{APFA}(k,m)$ in Eq. (3.2) is set within the transmission frequency band for the communication path. In the chaos analysis, the frequency of each subcarrier is handled at the $F_{APFA}(k,m)$ within the basic frequency band in Eq. (3.5).

The phase of the transmit signal $TX_{\sigma_{k,M}}(t)$ of APFA is expressed by a sum of exponential functions using a real part $\alpha_{\sigma_{k,M}}$ and an imaginary part $\beta_{\sigma_{k,M}}$ as follows;

$$e^{\alpha_{\sigma_{k,M}}(t)+j\beta_{\sigma_{k,M}}(t)} = \frac{1}{\sqrt{M}}\sum_{m=1}^{M} e^{j2\pi F_{APFA}(k,m)t}, \tag{4.1}$$

where k is the power root index of radical expression, and $\sigma_{k,M}$ is the normalized standard deviation of offset frequency between target frequency and APFA frequency.

Letting $t_n \equiv T_s \cdot n = 1/\Delta F \cdot n$ denote the discrete sampling time of each frame, (4.1) is expressed as follows:

$$e^{\alpha_{\sigma_{k,M}}(t_n)+j\beta_{\sigma_{k,M}}(t_n)} = \frac{1}{\sqrt{M}}\sum_{m=1}^{M} e^{j2\pi F_{APFA}(k,m)t_n}. \tag{4.2}$$

Therefore, $F_{APFA}(k,m)$ shown in Eq. (3.5) contains frequency component (f_m+$\Delta F/2$) as the periodic function part and the almost periodic frequency component part $\Delta F_{APFA}(k,m)$, $(1 \leq m \leq M)$ in the basic frequency band that is the same as $\Delta f(k,m)$ in the transmission frequency band,

$$F_{APFA}(k,m) = f_m + \Delta F/2 + \Delta f_{APFA}(k,m). \tag{4.3}$$

Since $(f_m - 0.5\Delta F)\cdot t_n = m\Delta F \cdot 1/\Delta F \cdot n = m \cdot n$ is an integer.

$$\beta_{\sigma_{k,M}}(t_n) = \arg\Big(\tfrac{1}{\sqrt{M}}\sum_{m=1}^{M} e^{j2\pi\Delta F_{APFA}(k,m)\cdot t_n}\Big). \tag{4.4}$$

The difference between the phase $\beta^1_{\sigma_{k,M}}(n)$ of signal 1 and the phase $\beta^2_{\sigma_{k,M}}$ of signal 2 at the point of $t = t_n$ is expressed by $\epsilon(n)$ as follows:

$$\epsilon(n) = \beta^1_{\sigma_{k,M}}(n) - \beta^2_{\sigma_{k,M}}(n), \quad n = 1, 2, \cdots. \tag{4.5}$$

Here, the frame Lyapunov exponent (FLE) is proposed to be defined by the following orbital sensitivity;

$$\lambda(n) = \frac{1}{n} \ln \left| \frac{\epsilon(n)}{\epsilon(0)} \right|, \quad n = 1, 2, \cdots, \tag{4.6}$$

where, $\epsilon(n)$ is the phase difference between signal 1 and signal 2 at frame number n, $\epsilon(0)$ is the phase difference between signal 1 and signal 2 at frame number 0.

The following transformations are performed to make it simple to calculate the local Lyapunov exponents in double-logarithms of (4.6) in case of finite interval.

$$\log_{10} \lambda(n) = -\log_{10} n + \log_{10} \ln \left| \frac{\varepsilon(n)}{\epsilon(0)} \right|, \quad n = 1, 2, \cdots. \tag{4.7}$$

4.1.1 Characteristics of FLE

We can say that there is orbital sensitivity if FLE is positive. However, FLE tends to decrease to zero as n increases; hence, short-term change is reduced to $1/n$.

In this section, we reveal the elucidation using the primary component (slope) Q_1, short-term variation $C(n)$ at frame number n, and stationary long-term parameter C_0 on the initial sensitivity of FLE.

The natural logarithm part of the Lyapunov exponent $\ln |\frac{\epsilon(n)}{\epsilon(0)}|$ is expressed by using Q_1, $C(n)$, and C_0 as follows:

$$C(n)C_0 n^{Q_1} \equiv \ln \left| \frac{\epsilon(n)}{\epsilon(0)} \right|, \quad n = 1, 2, \cdots. \tag{4.8}$$

Thus, the exponent of n is expressed by a function of $\log_{10} n$ with Q_1 as a parameter from (4.8) and (4.9).

$$\log_{10} \lambda(n) = (Q_1 - 1) \log_{10} n + \log_{10} C_0 C(n). \tag{4.9}$$

If we put $y(x) = \log_{10} \lambda(n),\ x = \log_{10} n$ and express it as a linear function of x of the form $y(x) = a_1 x + a_0$, then the short-term variation given by $C(n)$, fluctuations can be neglected in the long-term variation. Thus, when a_1 and a_0 are estimated, Q_1 and C_0 are determined as follows, $C_0 = 10^{a_0}$, $Q_1 = 1 + a_1$ using (4.10),

$$C(n) = 10^{\log_{10} \lambda(n) - (Q_1 - 1) \log_{10} n - \log_{10} C_0}, \quad n = 1, 2, \cdots. \tag{4.10}$$

By (4.10), the classification of the FLE can be as follows. If $Q_1 \geq 0$, then $\lambda(n)$ decreases slowly below the order of $1/n$.

1. $\lambda(n) > 0$ Unstable (initial value sensitive Chaos),

   $Q_1 \geq 0 :\ \lambda(n) = \mathcal{O}(\frac{1}{n^\gamma})\ \ (\gamma \leq 1)$,

   $Q_1 < 0 :\ \lambda(n) = \mathcal{O}(\frac{1}{n^\gamma})\ \ (\gamma > 1)$,

2. $\lambda(n) = 0$ Neutrality,

3. $\lambda(n) < 0$ Stability.

This category can be used to determine the orbit sensitivity of finite sections ($1 \leq n \leq N$). Figures 4.1 to 4.4 show FLE by double-logarithmic scales using simulation method.

The Q_1-value is changed by the standard deviation $\sigma^1_{k,M}$ of signal 1, and shows peak-value at $\sigma^1_{k,M}$ =0.005 and $\sigma^2_{k,M}$ =0.0001.

Table 4.1: Q_1-value for NOF standard deviation $\sigma^1_{k,M}$ at $\sigma^2_{k,M}$ =0.0001.

Items	$\sigma^1_{k,M}$	$\pi(N_a)$	a_1	Q_1	Reference
1	0.099	700	-0.921	0.079	Fig. 4.1
2	0.049	1230	-0.835	0.165	Fig. 4.2
3	0.01	8420	-0.879	0.121	Fig. 4.3
4	0.005	16935	-0.762	0.238	Fig. 4.4
5	0.003	28000	-0.9022	0.0978	–
6	0.0001	81000	-0.8875	0.1125	–

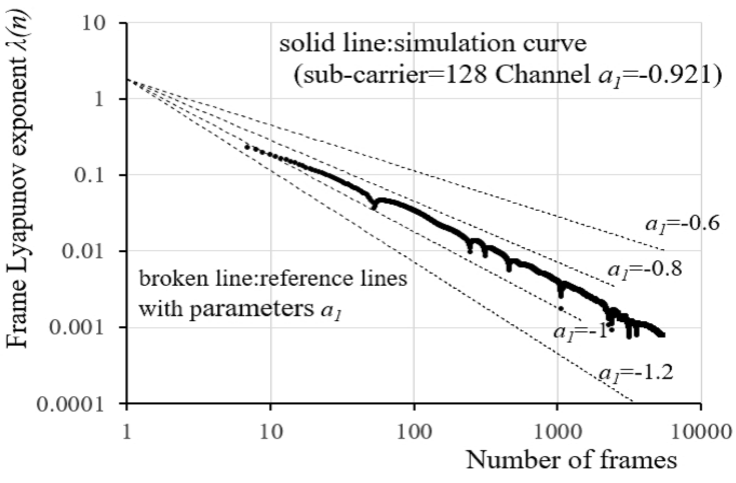

Figure 4.1: Frame Lyapunov exponent for frame number with $\sigma^1_{k,M}$ is being 0.099 and $\sigma^2_{k,M}$ being 0.0001 in the double-logarithm.
The broken lines show reference lines with the parameter $a_I being -0.6, -0.8, -1.0$, and -1.2, respectively as the same as Fig. 4.2 to Fig. 4.4.

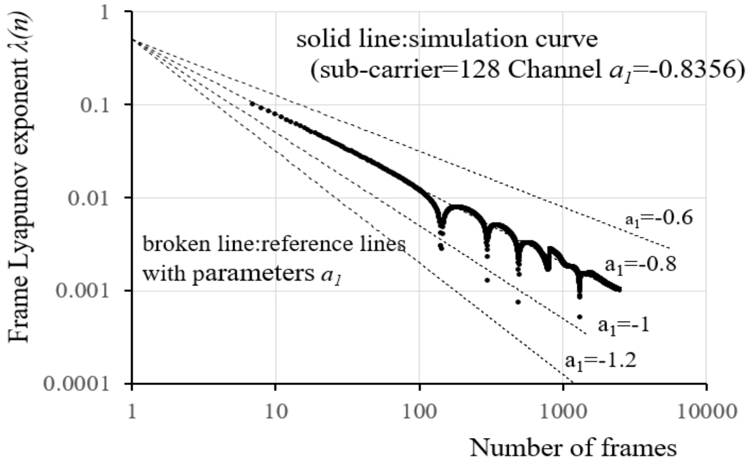

Figure 4.2: Frame Lyapunov exponent for frame number with $\sigma^1_{k,M}$ being 0.049 and $\sigma^2_{k,M}$ being 0.0001 in the double-logarithms scale.

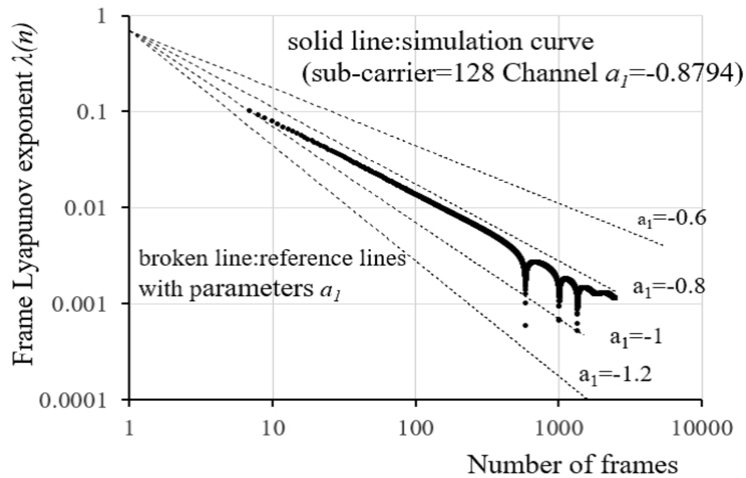

Figure 4.3: Frame Lyapunov exponent for frame number with $\sigma^1_{k,M}$ being 0.01 and $\sigma^2_{k,M}$ being 0.0001 in the double-logarithms scale.

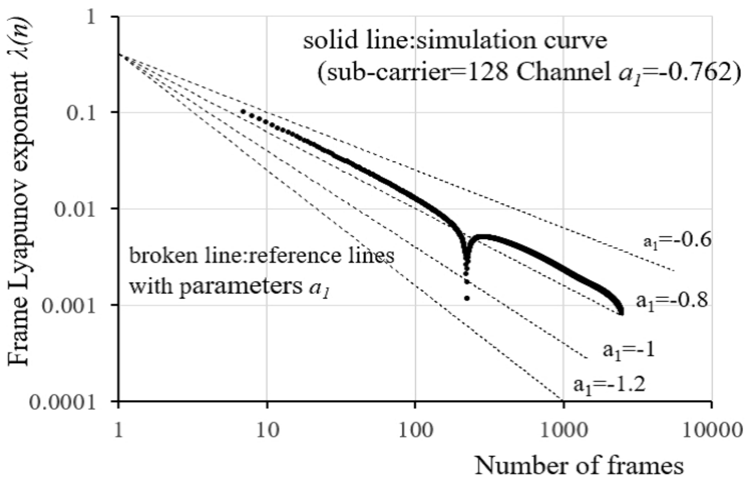

Figure 4.4: Frame Lyapunov exponent for frame number with $\sigma^1_{k,M}$ being 0.005 and $\sigma^2_{k,M}$being 0.0001 in the double-logarithms scale.

4.1.2 Short-Term Variation of FLE

The short-term variations $C(n)$ are obtained using (4.10) as shown in Fig. 4.5. Figure 4.5 exhibits the short-term variation, $C(n)$, of the Lyapunov exponent at $\sigma^1_{k,M}$=0.049. Even if the number of frames n is over than 100, the short-term variation is clearly expressed.

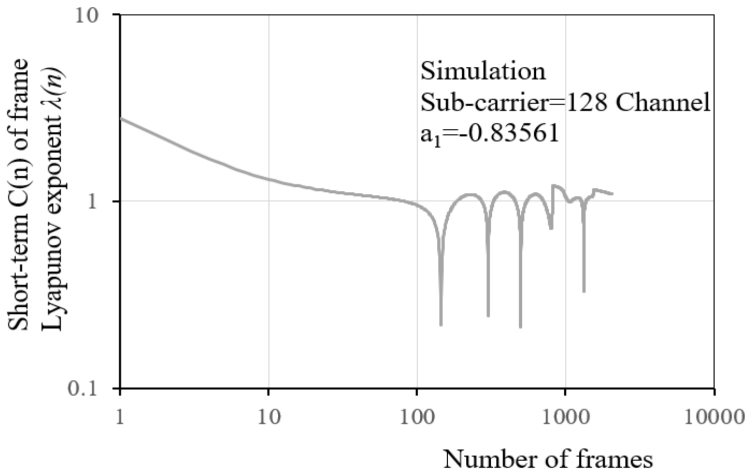

Figure 4.5: Frame Lyapunov exponent for frame number with $\sigma_{k,M}$ being 0.049.

4.2 Chaos-APFA (C-APFA)

4.2.1 Background

In the optical communication used for the trunk line, the line which bundles the branch line is required. Therefore, the communication capacity must be greater than or equal to Gbit/sec and greater than or equal to the Tbit/sec. The APFA system capable of 1,000,000 channel multiplexing for radio system has been shown in Chapter 2[15] This section proposes a scheme to aim the optical communication system or THz radio communication system, in which a wireless system of APFA is bundled.

4.2.2 Analysis Method to Create the Disjoint Set of Irrational Numbers

The APFA system of the radio system generates the almost periodic frequency arrangement by creating disjoint sets of numbers based on the prime number using the uniform distribution theorem by Weyl [9]. In order to obtain APFA, since the calculation time increases by prime numbers, we use the analysis method to create the disjoint sets of irrational numbers.

The Chebyshev function used in 2D exactly solvable chaos code is expressed by the following expressions.

$$(x_n, y_n) = (\cos m^{n-1}\theta, \sin m^{n-1}\theta), \tag{4.11}$$

where, θ is a initial phase (irrational number) and m is the order of Chebyshev function with $m \geq 2$.

The frequency group is created from the irrational number group that maps the level of x_n in Eq. (4.11) to the normalized frequency $(0 < f < 1)$. The probability mass function (PMF) of APFF frequency f of the Chebyshev function is then distributed to the interval $0 < f < 1$ in Fig. 4.6-(a) and is transformed to the uniform distribution (Fig. 4.6-(b)).

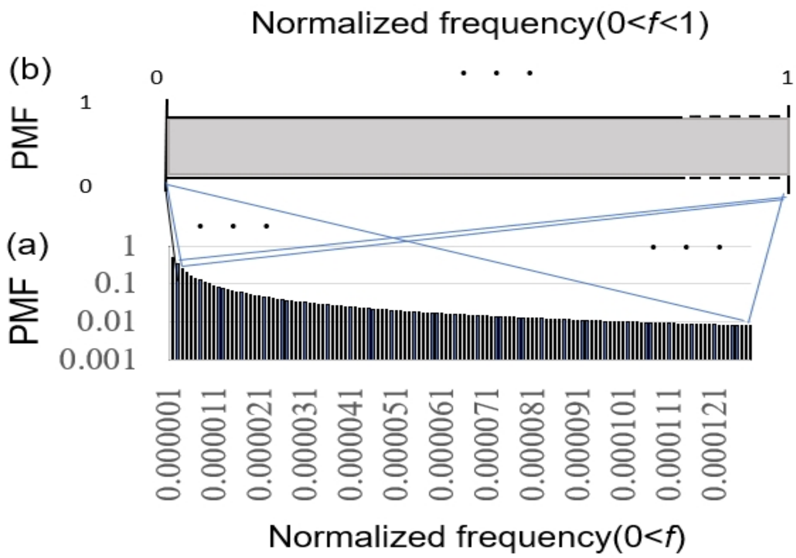

Figure 4.6: PMF Normalized frequency distribution.

We call this type of APFA system C-APFA. Figure 4.7 shows the normalized frequency standard deviation of the NOF for the number N of irrational numbers, and shows the comparison between the APFA and the C-APFA arrangement. Since its comparison is represented by the diagonal straight line, the C-APFA arrangement also has a uniform distribution.

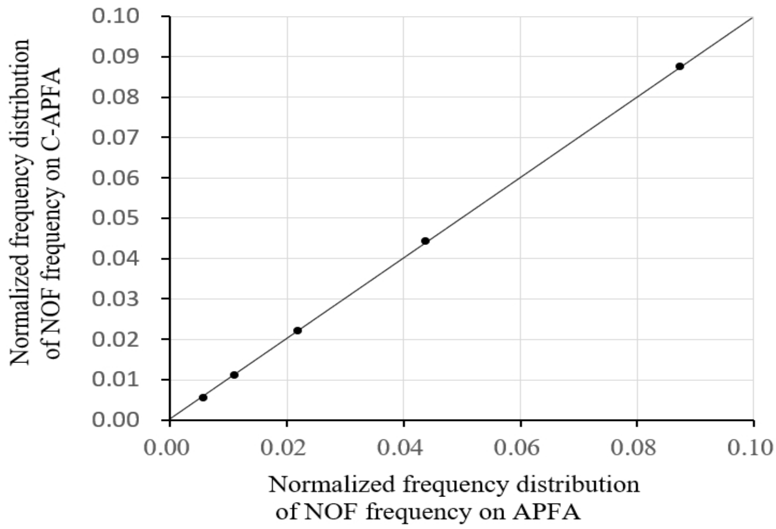

Figure 4.7: Comparison of the normalized standard deviation of NOF frequency APFA and C-APFA.

4.2.3 Frequency Probability Mass Function (PMF) of NOF

Figures 4.8, 4.9, and 4.10 show the frequency PMF of NOF for 16,384 CH subcarriers. As compared to the normal APFA, C-APFA has a feature that the NOF includes the *flat* area, the $1/f$ area, and the $1/f^A (A \geq 2)$ area.

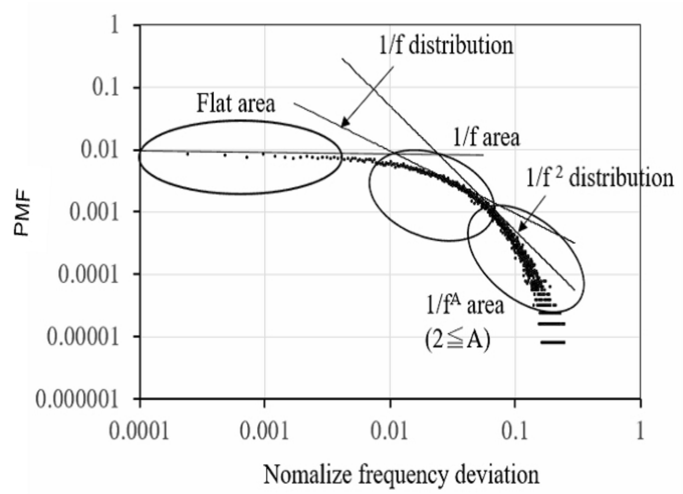

Figure 4.8: NOF frequency vs. PMF (C-APFA) with σ being 0.04423 and the number of subcarriers being 131,072.

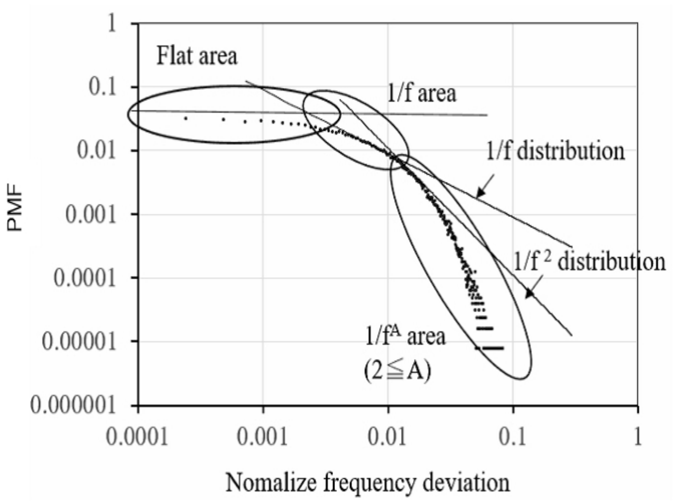

Figure 4.9: NOF frequency vs. PMF (C-APFA) with σ being 0.01104 and the number of subcarriers being 131,072,

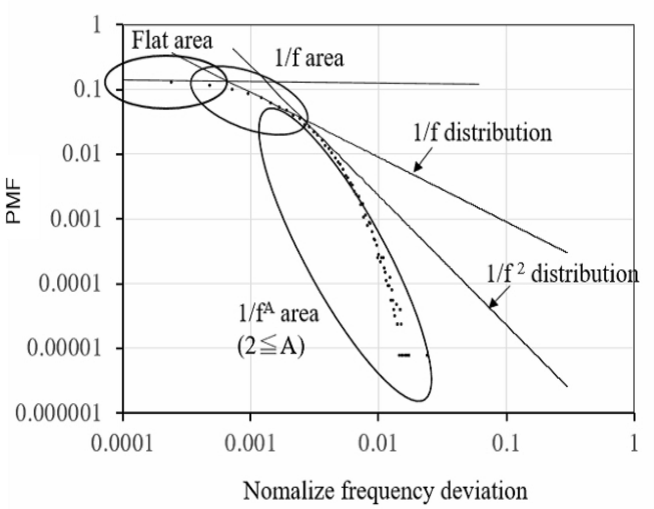

Figure 4.10: NOF frequency vs. PMF (C-APFA) with σ being 0.00231 and the number of subcarriers being 131,072.

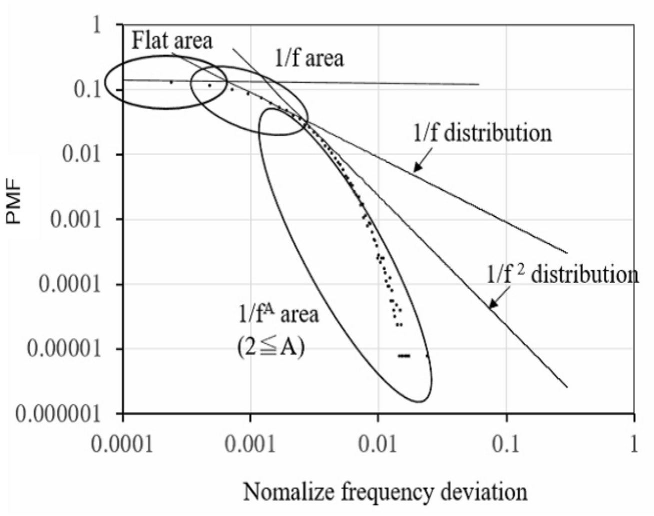

Figure 4.11: NOF frequency vs. PMF (C-APFA) with σ being 0.00231 and the number of subcarriers being 131,072.

4.2.4 Characteristics of FLE

Figure 4.12, 4.13, 4.14, 4.15, 4.16 show the FLE of C-APFA calculated in the same manner as the APFA.

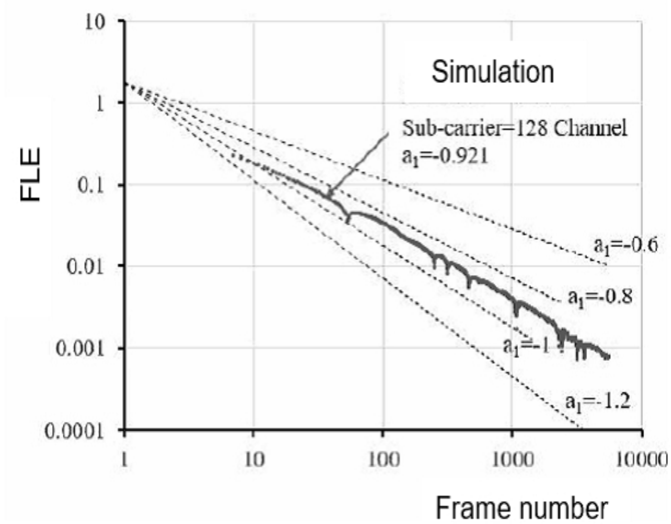

Figure 4.12: Frame Lyapunov exponent for frame number with $\sigma^1_{k,M}$ being 0.098 and $\sigma^2_{k,M}$ being 0.0001 in the double-logarithms scale.

Table 4.2 shows the Q values using the slope a_1 obtained from Fig. 4.12 to 4.16. Here, when $\sigma^1_{k,M} = 0.005$, the maximum initial value sensitivity is shown.

Table 4.2: Q_1-values for NOF standard deviation $\sigma^1_{k,M}$ at $\sigma^2_{k,M}$ =0.0001.

Items	Fig. 4.12	Fig. 4.13	Fig. 4.14	Fig. 4.15	Fig. 4.16
$\sigma^1_{k,M}$	0.098	0.049	0.01	0.005	0.00013
a_1	-0.921	-0.835	-0.870	-0.762	-0.8846
Q_1	0.079	0.165	0.130	0.238	0.1154

Fig. 4.17 shows the curves in the standard deviation σ of the normalized offset frequency (NOF) close to the OFDM frequency of the C-APFA target relative to the number of irrational numbers, for 6 million subcarrier channels, which is approximately $threetimesof2millionchanelso$

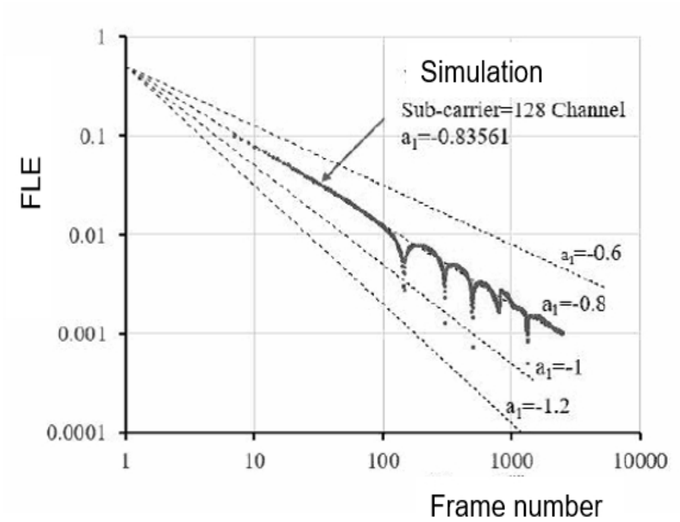

Figure 4.13: Frame Lyapunov exponent for frame number with $\sigma^1_{k,M}$ being 0.049 and $\sigma^2_{k,M}$ being 0.0001 in the double-logarithms scale.

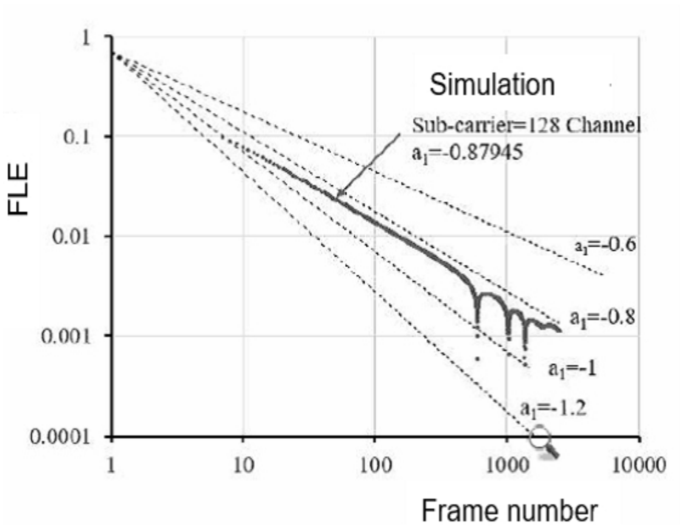

Figure 4.14: Frame Lyapunov exponent for frame number with $\sigma^1_{k,M}$ being 0.01 and $\sigma^2_{k,M}$ being 0.0001 in the double-logarithms scale.

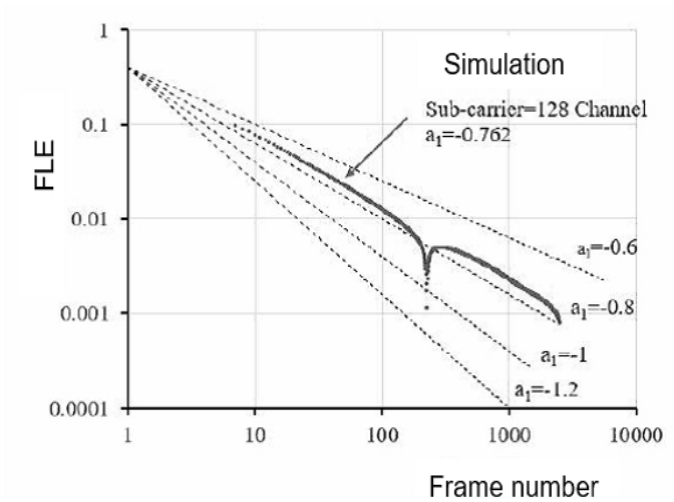

Figure 4.15: Frame Lyapunov exponent for frame number with $\sigma_{k,M}^1$ being 0.005 and $\sigma_{k,M}^2$ being 0.0001 in the double-logarithms scale.

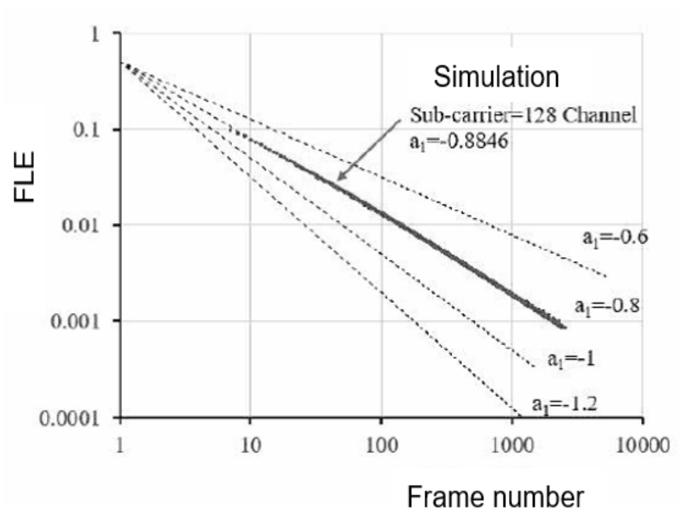

Figure 4.16: Frame Lyapunov exponent for frame number with $\sigma_{k,M}^1$ being 0.0013 and $\sigma_{k,M}^2$ being 0.0001 in the double-logarithms scale.

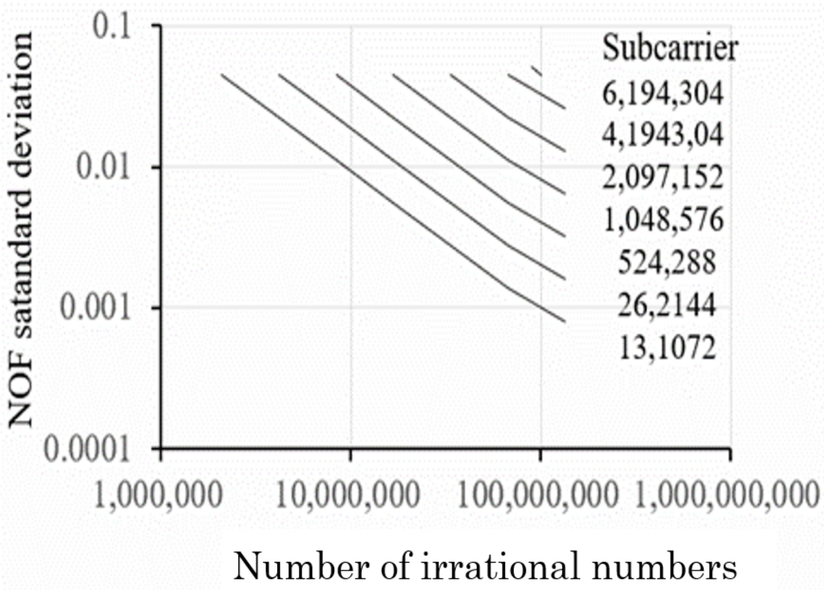

Figure 4.17: NOF standard deviation σ for the number of irrational numbers
(The numbers of subcarriers: $13,1072 \sim 6,194,304$ channels)
(Chebyshev function with the parameter $\theta = \sqrt[3]{71}$ and $m = 7$.)

.

4.3 Conclusions

By using FLE, we feature the chaotic property of the APFA signals in which frequencies are allocated from the normalized irrational frequency group by linearly mapping the irrational number group, which comprises the power root of a prime number. We show new concept of Chaos-APFA (C-APFA) that enables subcarrier frequency allocation with up to *six million channels* and then elucidate chaotic property using computer simulations.

Chapter 5

Applications of APFA

Three examples are given in which the APFA method is applied to other than satellite communication and mobile communication.

5.1 Small Scale APFA

Here in this chapter we consider small scale APFA with small number of subcarriers. We simulated a phase jump on the phase diagram of the transmission signal as a characteristic related to the synchronization system of small-scale APFA communication.

Figure 5.1 shows the phase difference (degrees) of the received wave when the number of subcarriers = 32, σ= 0.01, and there is almost no jump in the phase difference, but whe n the number of subcarriers= 32, σ = 0.12, many phase difference jumps are seen as in Fig. 5.2. When σ becomes 0.05 to 0.1, the number of peaks of the phase difference of the received wave increases and the phase of the received signal becomes unstable. Fig. 5.3 shows the results of the simulation under the same conditions as in Fig. 5.2, and the peak value of the phase difference of the received wave is obtained by changing the normalized standard deviation σ. It can be seen that when σ becomes 0.05 to 0.1, the peak value of the phase difference of the received wave increases and a jump of about 180 degrees may occur in Fig. 5.4.

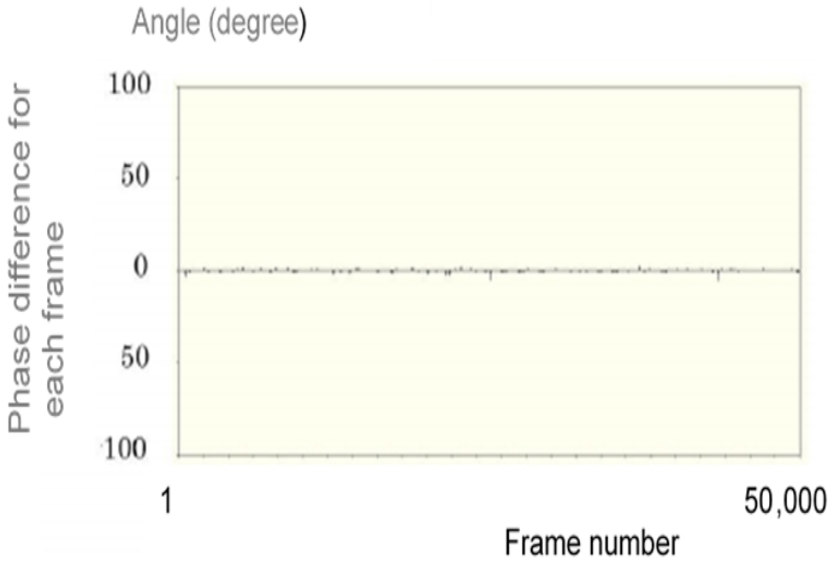

Figure 5.1: Phase difference (degree) of the received wave compared to the normalized standard deviation of the NOF (the number of subcarriers = 32, σ = 0.01).

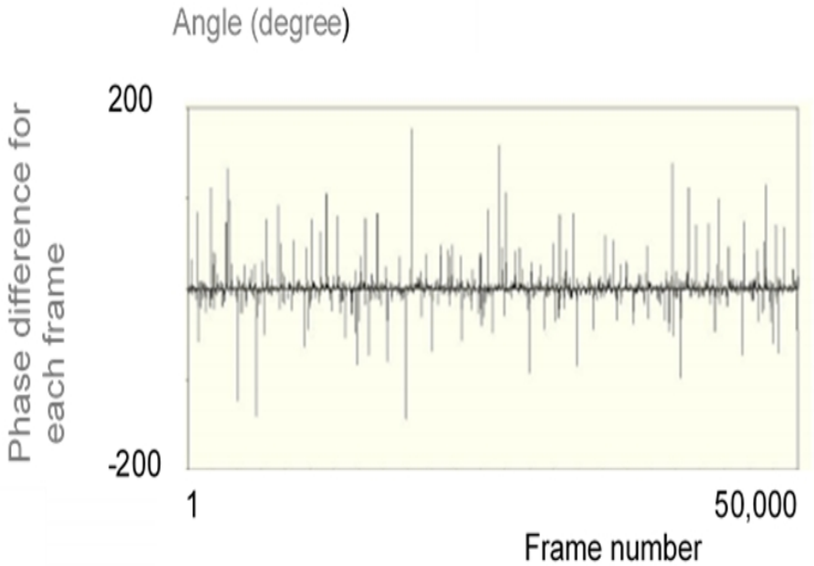

Figure 5.2: Phase difference (degree) of the received wave compared to the normalized standard deviation of the NOF (the number of subcarriers = 32, σ = 0.129).

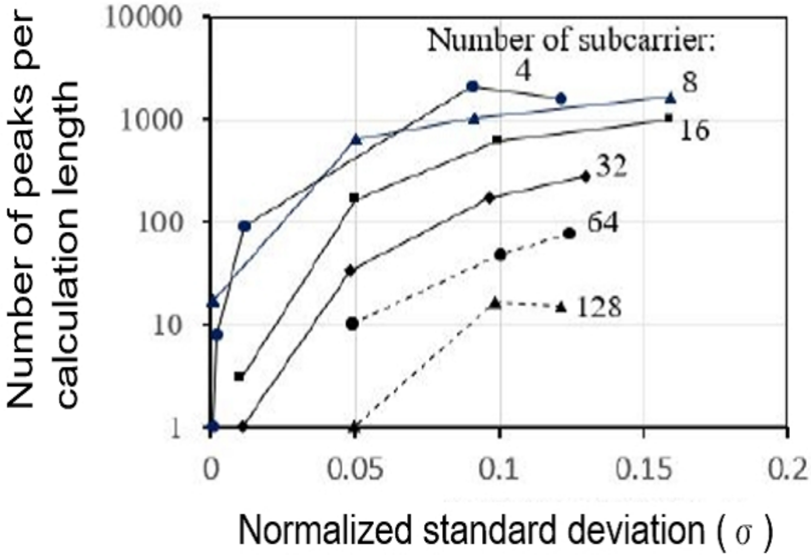

Figure 5.3: The number of peaks of the phase difference of the received wave with respect to the normalized standard deviation of NOF.

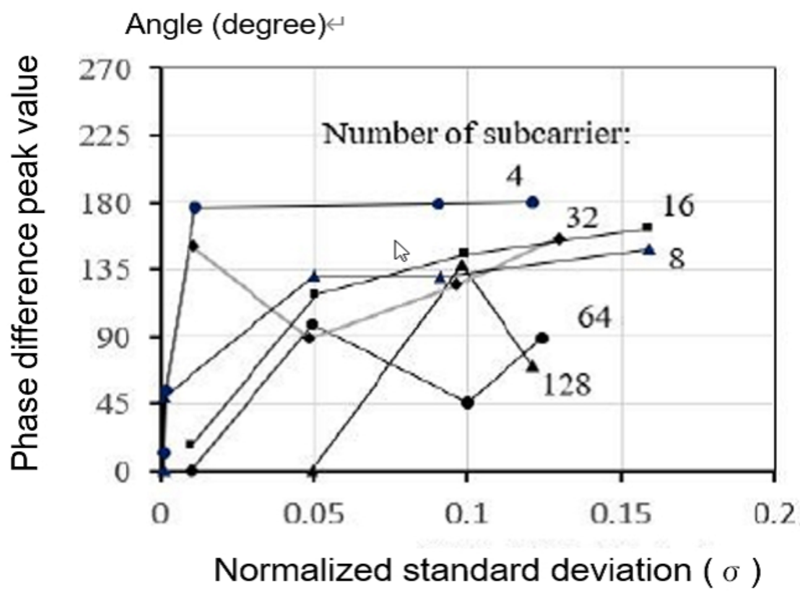

Figure 5.4: The maximum peak value of the phase difference of the received wave with respect to the normalized standard deviation of NOF.

5.2 Seamless Satellite Communication System

It is required to provide more advanced broadcasting services using ultra-high-definition video technology (4K, 8K) of terrestrial digital broadcasting. In addition, it is urgent to conduct R & D on a 5-th and beyond 5-th generation mobile communication system that has high spectrum efficiency, high speed and high capacity communication, and so on.

The proposed seamless system here is related to signal processing using super-multiplexing on the frequency axis. By deploying the APFA system into the real communication system, wireless terminals can be seamlessly communicated between terminals via seamless relay, repeaters, and communication/broadcasting systems as shown in Fig. 5.5.

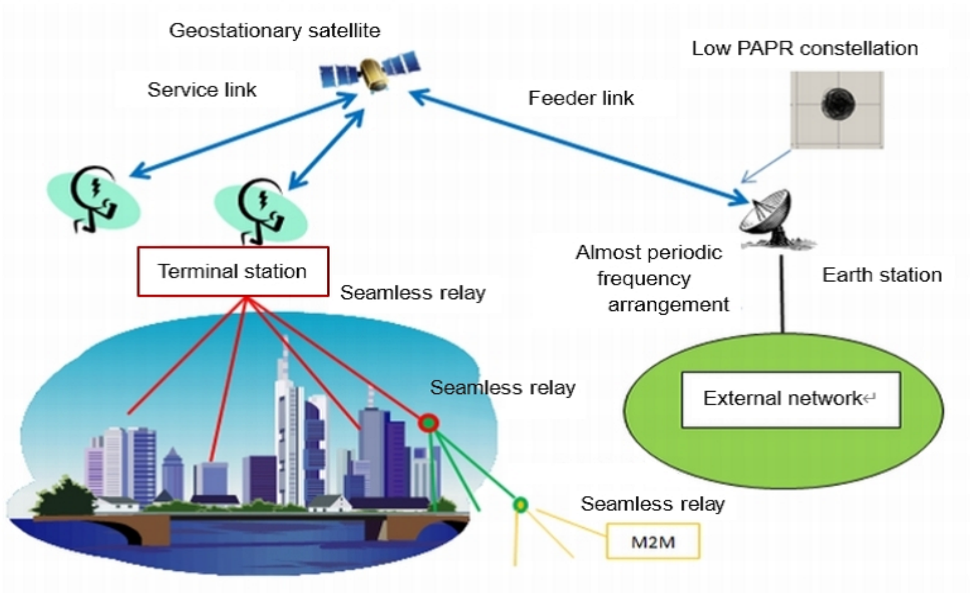

Figure 5.5: Seamless satellite communication system.

5.3 APFA Ultra Wide Band Wireless Communication (APFA-UWB)

Ultra wide band wireless communication (UWB) is an advantageous method for identifying the position of the device, because it is a communication method using an impulse signal as well as an ultra-high-speed transmission.

However, although the UWB communication system has a small transmission power per frequency, the UWB system is a radio system using an impulse, so the frequency bandwidth to be used is an extremely wide range from 500 MHz to several GHz and the interference to an existing radio system is unavoidable.

The APFA-UWB method in this research is a proposal to utilize the positioning features of the conventional UWB method in the system of APFA RF carrier siganl generation and to use it as a method to solve the interference characteristics, which can be regarded as a disadvantage.

This APFA-UWB system presents an outline of an impulse communication system in an ultra-wideband frequency band by using an approximate frequency function which makes the carrier frequency asynchronous.

The frequency spectrum that can be used for the microwave band UWB are defined by the power mask shown in Fig. 5.6.

Since the spectrum efficiency of the APFA-UWB system is high, it is easy to satisfy the power mask in Fig. 5.6 by controlling the level of subcarriers,

Figure 5.7 shows a synthesized wave using APFA-UWB system. A synthesized wave (OFDM) by the periodic function shown in Fig. 5.8 shows a periodic characteristic on the time axis. On the other hand, APFA system has a characteristic that the peak value of each frame decreases on the time axis. If a synthesized signal of APFA at frame after a long time is used, it is the signal dispersed on the time axis and the frequency axis, and can be used for communication of an impulse signal and distance measurement.

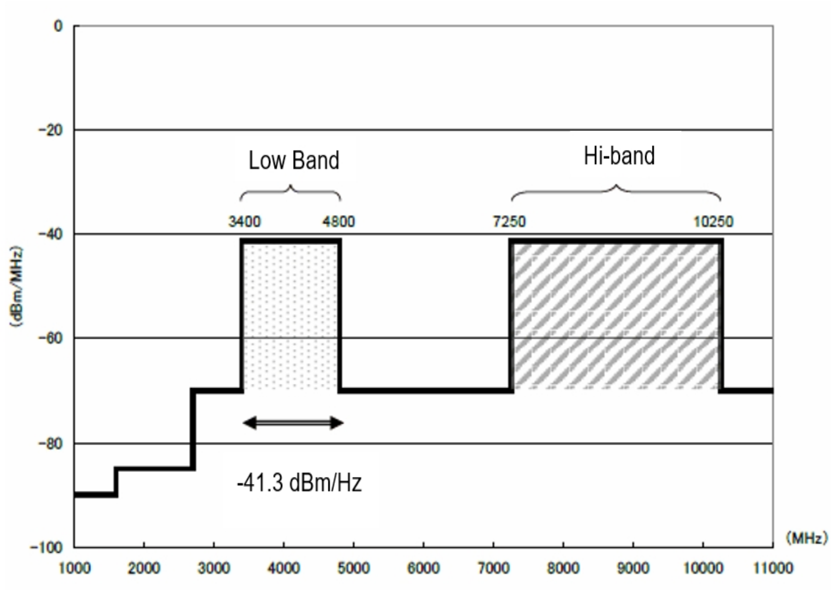

Figure 5.6: Domestic UWB system power mask (indoor) in Japan [22].

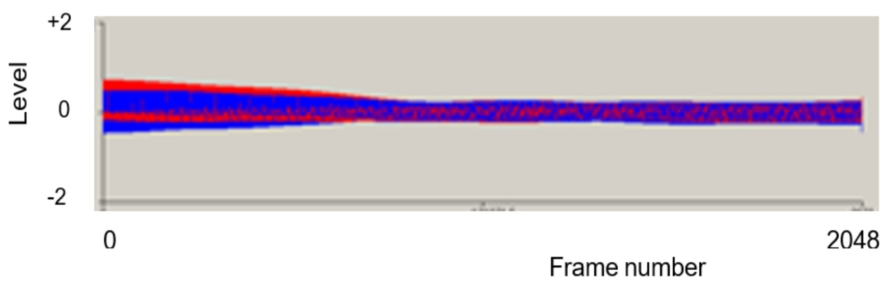

Figure 5.7: Synthesized wave by APFA-UWB.

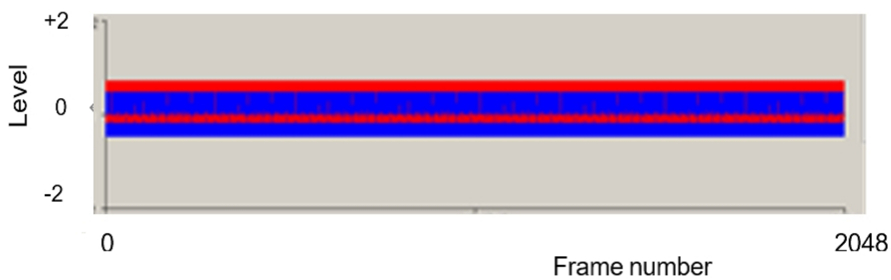

Figure 5.8: Synthesized wave by OFDM.

Chapter 6

Conclusions

6.1 Motivation for APFA

The motivation for APFA research is to solve the problems that must be overcome on the satellite communications, such as 1) the effects of the nonlinearity of the power amplifier, and 2) the high crest factor in the frequency separation multiplexing system.

6.2 APFA scheme

We discuss the APFA scheme on the premise of Hilbert space L^2 for a disjoint set of irrational numbers.
It is possible to cut the irrational number group using rational numbers at any time when the irrational numbers show a uniform distribution. Thus, it is also possible to construct an APFA scheme using an irrational number group that is guaranteed by a Weyl's uniform distribution theorem.
We propose the almost periodic frequency arrangement (APFA) with asynchronous method for satellite communications using the high frequency multiplexing on computer simulation system. We also show the new concept of APFA that enables subcarrier frequency allocation with up to several million channels and the basic performance using computer simulations. Regarding the above problem 1), the composite wave of each subcarrier of the intermodulation product of APFA is power sum, so it is more advantageous than OFDM, which is basically a voltage sum of OFDM explained in section 2.4. Regarding the above problem 1), we have developed a technique for

suppressing the normalized values on the complex space explained in Section 2.6. Although APFA is an asynchronous communications, the BER characteristic exhibits a value similar to the theoretical value by performing complex synchronization detection.

6.3 Frame Lyapunov exponent

We propose a new frame Lyapunov exponent (FLE) which can estimate the phase difference sensitivity depending on the frame number in APFA. By using FLE, we feature the chaotic property of the APFA signals in which frequencies are allocated from the normalized irrational frequency group by linearly mapping the irrational number group, which comprises the power root of a prime number. We reveal the universal feature of FLE that the frame Lyapunov exponent $\lambda(n)$ has the power law such as $\lambda(n)=\mathcal{O}(\frac{1}{n^{\gamma}})$ with $\gamma > 0$ and the exponent γ depends on the standard deviation $\sigma_{k,M}$ of the normalized offset frequency (NOF) at APFA system. By using FLE, we feature the chaotic property of the APFA signals in which frequencies are allocated from the normalized irrational frequency group by linearly mapping the irrational number group, which comprises the power root of a prime number.

6.4 Chaos-APFA

We propose Chaos-APFA (C-APFA) system using 2D exactly solvable chaos code to aim the optical communication system or THz radio communication system. We also show new concept of C-APFA that enables subcarrier frequency allocation of up to six million channels and chaotic property using computer simulations. In the future we plan to analyze future problem with the aim of the performance which can be applied to diversification and the large capacity in satellite communications.

Bibliography

[1] M. Pätzold, 5G Sets Around the Globe, *IEEE Vehicular Technology Mag.*, **14**, (2019), 5-11.

[2] 3rd Generation Partnership Project,Technical Specification Group Services and System Aspects;3GPP Release 15 Description, *TR 21.915*, V0.6.0, pp. 21, Feb., 2019

[3] Visit https://itsforum.gr.jp/Public/J3Schedule/P10/j6_housou.pdf

[4] Visit https://www.tele.soumu.go.jp/resource/search/myuse/use/335m.pdf

[5] K. Umeno, On Complex Spreading Sequence with Constant Power and Exact Orthogonality for Chaos-CDMA : Integration of OFDM and CDMA via Chaos-CDMA, *IEICE Technical Report*, NLP2008-37, (2008), 23-27.

[6] Ken Umeno, Independent Component Analysis of Chaotic Mixtures and Chaotic Analysis, *Laser Society of Japan*, vol. 39, (2011), 488-494 (In Japanese).

[7] K. Umeno, Spread Spectrum Communications Based on Almost Periodic Functions : Almost Periodic Code Approach versus Chaotic Code Approach for Communications. *IEICE Technical Report*, **114**, NLP2014-62, (2014), 87-90, (In Japanese).

[8] Tomoya Naohara, Ken Umeno, Performance Analysis of Super Dense Multiple Access (SDMA) Communications Systems Using Almost Periodic Function Codes, *IEICE Technical Report*, NLP2014-101, pp. 11-16, Dec. 2014, (In Japanese).

[9] H.Weyl, Uber die Gleichverteilung von Zahlen mod. Eins, *Mathematishe Annalen*, volume 77, pp.313-352, 1916.

[10] T. Takagi, Mathematical analysis, *Iwanami Shoten*, Revised edition 3, (1969), (In Japanese).

[11] K, Matuzaka, A course in analysis, *Iwanami Shoten*, First edition, (1997), (In Japanese).

[12] I. Nakazawa and K. Umeno, Almost periodicity frequency arrangement and application to satellite communication system, *IEICE Technical Report*, **115**, CCS2015-33, (2015), 23-26, (In Japanese).

[13] I. Nakazawa and K. Umeno, Applicability and characteristics to satellite communications with power constant chaotic spreading sequence, *IEICE Technical Report*, **115**, CCS2015-28, (2015), 73-78, (In Japanese).

[14] I. Nakazawa and K. Umeno, Performance Evaluation of Wideband Radio Communication Systems using Almost Periodic Frequency Arrangement, *Proc. of ICSGTEIS 2016*, pp. 673-678, Bali, Oct. 2016. DOI:10.1109/ICSGTEIS.2016.7885765

[15] I. Nakazawa and K. Umeno, Fundamental study on almost periodic frequency arrangements for super-multi-access radio communication systems, *IEICE Communication Express*, **1**, 1-6, (2017), DOI:10.1587/comex.2017XBL0135

[16] I. Nakazawa and K. Umeno, Application and Chaotic Feature of APFA (New Concept) to Optical Communication, *The 530th Topical Meeting of The Laser Society of Japan*, No.RTM-19-01-04, (2019), 19-24, (In Japanese).

[17] I. Nakazawa and K. Umeno, Chaotic property of almost periodic frequency arrangement (APFA), *JSIAM Letters*, **12**, 9-12, (2020).

[18] A. Ishizawa, etc., "Ultralow-phase-noise millimetre-wave signal generator assisted with an electro-optics-modulator-based optical frequency comb," *Scientific Reports*, volume 6, Article number: 24621 (2016)

[19] Saed V. Vaseghi, *Advanced Digital Signal Processing and Noise Reduction*, WILEY,p.p 35 to 39, Forth Edition, 2008

[20] I. Nakazawa and K. Umeno, Almost periodicity frequency arrangement and application to satellite communication system, *IEICE Technical Report* , CCS2015-33, 23-26, 2015,

[21] I. Nakazawa, K. Umeno, Performance evaluation of satellite communication system using almost periodic frequency arrangement *IEICE Technical Report*, CCS2015-59, 75-78, 2015.

[22] I. Nakazawa and K. Umeno, Impulse Communications by Almost Periodic Frequency Arrangements), *JSIAM2015 General Meeting*, 2015.

[23] I. Nakazawa and K. Umeno, New communication form and application using a non-periodic function (based on irrational number), *NICT Time and Space Conference*, 2016.

[24] I. Nakazawa and K. Umeno, Seamless communication and broadcasting technology based on signal processing of almost periodic frequency, *NICT*

Space communication system 39th Conference, 2016.

[25] I. Nakazawa and K. Umeno,Study of satellite communication with a non-periodic function. *Kyoto University 10th ICT innovation*, (2016), (In Japanese).

[26] I. Nakazawa and K. Umeno, Electromagnetic wave space identification method to use infinity length cycle function, *Kyoto University 10th ICT innovation*, 2016. (In Japanese).

[27] I. Nakazawa and K. Umeno, Wideband wireless communication using the almost periodic chaos code, *JSIAM2016 12th General Meeting*,B211, 2016.

[28] I. Nakazawa and K. Umeno, Chaotic properties in APFA communication, *JSIAM2018 General Meeting*, 77-78, 2018.

[29] I. Nakazawa and K. Umeno, Wireless group power transmission system using frequency multiplexing, （Almost periodic frequency arrangement (APFA) method） *JSIAM2019 General Meeting*, 160-161, 2019.

[30] I. Nakazawa and K. Umeno, The application of satellite communication equipment signal processing and chaos code aimed at high-quality, *NICT Applied Electromagnetic Research Institute Exchange meeting 2014*, (2014).

[31] I. Nakazawa and K. Umeno, Application to satellite communication using almost periodic frequency arrangement, (application of irrational and almost peridic signals) *NICT Applied Electromagnetic Research Institute Exchange meeting2015*, (2015).

[32] I. Nakazawa and K. Umeno, Seamless communication and broadcasting technology based on signal processing of almost periodic frequency. *Kyoto University 10th ICT Innovation*, 2016.

[33] I. Nakazawa and K. Umeno, Electromagnetic wave space identification method to use infinity length cycle function, *Kyoto University 10th ICT Innovation*, 2016.

[34] I. Nakazawa and K. Umeno, Application of almost periodic frequency assignment to C-PLANE network *JSIAM2016 General Meeting*, 2016.

[35] I. Nakazawa and K. Umeno, Chaotic property and applicability for wireless communication systems using almost periodic frequency arrangement (APFA) based on irrational numbers, *Kyoto University 14th ICT Innovation*, 2019.

[36] Kadowaki Naoto and Suzuki Ryutaro, 2 Overview of the Wideband InterNetworking Engineering Test and Demonstration Satellite ProjectApplication of almost periodic frequency *Journal of the National Institute of Information and Communications Technology Vol.54 No.4* , 2007.

[37] Hamamot Naokazu, Yoshimoto Shigetoshi, and Imae Michito, 2 Overview of the Engineering Test Satellite VIII (ETS-VIII) Project, *Journal of the National Institute of Information and Communications Technology Vol.50 Nos.3/4* , 2003.

[38] 5GMF: White paper, 5G Mobile Communications Systems for 2020 and beyond, Ver1.1 (September 29, 2017),
Visit: https://5gmf.jp/whitepaper/5gmf-white-paper-1-1/.

[39] Recommendation ITU-R M.2083-0(09/2015), IMT Vision-Framework and overall objectives of the future development of IMT for 2020 and beyond.

[40] Yoshida Susumu, Sato Kohei, Nakamura Takehiro, Recent Trend of Mobile Communications : What is Going on in ITS World? *IEICE, 101, 11* , 2018.

[41] K. Umeno, Advanced Institute for Complex Systems, *Information Systems as Complex Systems*, KYORITSU SHUPPAN, The Complex Systems Monograph Series Vol. 4, (2007), (In Japanese).

[42] Y. Saito, Digital modulation technique for wireless communications, *IEICE*, CORONA SHUPPAN, (1996), (In Japanese).

List of reviewed papers

[1] I. Nakazawa and K. Umeno, Fundamental study on almost periodic frequency arrangements for super-multi-access radio communication systems, *IEICE Communication Express*, **1**, 1-6, (2017), DOI:10.1587/comex.2017XBL0135

[2] I. Nakazawa and K. Umeno, Chaotic property of almost periodic frequency arrangement (APFA), *JSIAM Letters*, **12**, 9-12 (2020).

[3] I. Nakazawa and K. Umeno, New Concept and Performance of Wideband Satellite Communication Systems using Almost Periodic Frequency Arrangement, *IEICE Trans. Commun.*, (submitted).

[4] I. Nakazawa and K. Umeno, Chaotic Feature of Almost periodic frequency arrangement (APFA) , *THE LASER SOCIETY OF JAPAN*, (submitted), (in Japanese).

Conference

[1] I. Nakazawa and K. Umeno, Performance Evaluation of Wideband Radio Communication Systems using Almost Periodic Frequency Arrangement, *Proc. of ICSGTEIS 2016(IEEE)*, pp. 673-678, Bali, Oct. 2016, DOI:10.1109/ICSGTEIS.2016.7885765.

APFA Oral presentation

[1] I. Nakazawa and K. Umeno, Almost periodicity frequency arrangement and application to satellite communication system, *IEICE Technical Report* , CCS2015-33, 23-26, 2015,

[2] I. Nakazawa and K. Umeno, Applicability and characteristics to satellite communications with power constant chaotic spreading sequence, *IEICE Technical Report*, CCS2015-13, 73-76, 2015,

[3] I. Nakazawa and K. Umeno, Almost periodicity frequency arrangement and application to satellite communication system, *IEICE Technical Report*, CCS2015-33, 23-26, 2015,

[4] I. Nakazawa, K. Umeno, Performance evaluation of satellite communication system using almost periodic frequency arrangement *IEICE Technical Report*, CCS2015-59, 75-78, 2015.

[5] I. Nakazawa and K. Umeno, Impulse Communications by Almost Periodic Frequency Arrangements), *JSIAM2015 General Meeting*, 2015.

[6] I. Nakazawa and K. Umeno, New communication form and application using a non-periodic function (based on irrational number), *NICT Time and Space Conference*, 2016.

[7] I. Nakazawa and K. Umeno, Study of satellite communication with a non-periodic function. *NICT Space communication system 39th Conference*, 2016.

[8] I. Nakazawa and K. Umeno, Seamless communication and broadcasting technology based on signal processing of almost periodic frequency, *Kyoto University 10th ICT innovation*, (2016), (In Japanese).

[9] I. Nakazawa and K. Umeno, Electromagnetic wave space identification method to use infinity length cycle function, *Kyoto University 10th ICT innovation*, 2016. (In Japanese).

[10] I. Nakazawa and K. Umeno, Wideband wireless communication using the almost periodic chaos code, *JSIAM2016 12th General Meeting*,B211, 2016.

[11] I. Nakazawa and K. Umeno, Chaotic properties in APFA communication, *JSIAM2018 General Meeting*, 77-78, 2018.

[12] I. Nakazawa and K. Umeno, Application and Chaotic Feature of APFA (New Concept) to Optical Communication, *The 530th Topical Meeting of The Laser Society of Japan*, No.RTM-19-01-04, 19-24, 2019.

[13] I. Nakazawa and K. Umeno, Wireless group power transmission system using frequency multiplexing, （Almost periodic frequency arrangement (APFA) method） *JSIAM2019 General Meeting*, 160-161, 2019.

APFA Panel presentation

[1] I. Nakazawa and K. Umeno, The application of satellite communication equipment signal processing and chaos code aimed at high-quality, *NICT Applied Electromagnetic Research Institute Exchange meeting 2014*, (2014).

[2] I. Nakazawa and K. Umeno, Application to satellite communication using almost periodic frequency arrangement, (application of irrational and almost peridic signals) *NICT Applied Electromagnetic Research Institue Exchange meeting 2015*, (2015).

[3] I. Nakazawa and K. Umeno, Seamless communication and broadcasting technology based on signal processing of almost periodic frequency. *Kyoto University 10th ICT Innovation*, 2016.

[4] I. Nakazawa and K. Umeno, Electromagnetic wave space identification method to use infinity length cycle function, *Kyoto University 10th ICT Innovation*, 2016.

[5] I. Nakazawa and K. Umeno, Application of almost periodic frequency assignment to C-PLANE network *JSIAM2016 General Meeting*, 2016.

[6] I. Nakazawa and K. Umeno, Chaotic property and applicability for wireless communication systems using almost periodic frequency arrangement (APFA) based on irrational numbers, *Kyoto University 14th ICT Innovation*, 2020.

Awards

1. ARIB The Award of the Chairman of the Board of ARIB in 2004.
2. THE LASER SOCIETY OF JAPAN Laser Chaos OOTUBO Award in 2020.

Patents

1. Patent application number: 2017-522286
International Publication Number: WO2016195085 in 2015